

The role of physical factors in photodegradation of polypropylene

Radka Mošnovská

Master Thesis
2007



Univerzita Tomáše Bati ve Zlíně
Fakulta technologická

nascannované zadání s. 1

nascannované zadání s. 2

ABSTRAKT

Diplomová práce se zabývá vlivem některých fyzikálních faktorů, jako jsou tloušťka materiálu nebo způsob jeho zpracování, na fotodegradaci izotaktického polypropylenu.

Vzorky byly připraveny lisováním nebo vstřikováním a následně v laboratorních podmínkách vystaveny UV záření. Rozsah degradace byl určován za použití infračervené spektroskopie s Fourierovou transformací (FTIR) nebo za použití techniky infračervené spektroskopie se zeslabenou úplnou reflektancí (ATR). Dále byl zkoumán degradační profil lisovaných vzorků metodou mikro-infračervené spektroskopie.

Klíčová slova: Izotaktický polypropylen, fotodegradace, fyzikální faktory, tloušťka, zpracování, degradační profil.

ABSTRACT

Master thesis is focused on the role of physical factors such as thickness or mode of processing in photodegradation of isotactic polypropylene. Specimens were prepared by compression moulding or injection moulding. Subsequently, they were exposed to UV radiation in accelerated ageing device. The extent of degradation was determined by using Fourier transform infrared spectroscopy (FTIR) or attenuated total reflection infrared spectroscopy (ATR). Next, the degradation profile of compression-moulded specimens was observed by micro-infrared spectroscopy.

Keywords: Isotactic polypropylene, photodegradation, physical factors, thickness, processing, degradation profile.

ACKNOWLEDGEMENTS

First of all, I would like to thank to my supervisor Ing. Roman Čermák, PhD. for initiating of this work, for suggestive advice within the master thesis formation and for supporting during my stay in Clermont-Ferrand.

My sincere gratitude belongs to Prof. Sophie Commereuc and Prof. Vincent Verney from Blaise Pascal University for leading through the problems that occurred during composition of this master thesis, valuable advice and help with experiments.

My thanks belong to teachers and graduants from the Laboratory of molecular and macromolecular photochemistry in Clermont-Ferrand.

I am grateful to my parents to make my studies possible and I would also like to thank to my boyfriend Henry for continuous support and encouragement.

I declare, I worked on this Master Thesis by myself and I mentioned all the used literature.

Zlín, 10th May, 2007

Radka Mošnovská

CONTENTS

INTRODUCTION	6
I STATE-OF-THE-ART	8
1 POLYPROPYLENE	9
1.1 POLYMERIZATION REACTION.....	10
1.2 STRUCTURE OF POLYPROPYLENE.....	10
1.2.1 Atactic polypropylene	11
1.2.2 Syndiotactic polypropylene.....	12
1.2.3 Isotactic polypropylene	13
1.3 POLYMORPHISM OF ISOTACTIC POLYPROPYLENE.....	14
1.3.1 α -form.....	16
1.3.2 β -form.....	17
1.3.3 γ -form.....	18
1.3.4 Smectic form	19
1.4 PROPERTIES OF POLYPROPYLENE.....	19
1.5 MORPHOLOGY ASSOCIATED WITH PROCESSING	19
1.5.1 Skin-Core and related morphologies.....	20
1.5.1.1 Impact of injection moulding on morphology of polymers.....	20
1.5.1.2 Impact of compression moulding on morphology of polymers.....	21
2 DEGRADATION.....	22
3 PHOTODEGRADATION	24
3.1 LIGHT SOURCE.....	24
3.2 ELECTROMAGNETIC RADIATION	24
3.3 IMPACT OF ULTRAVIOLET RADIATION ON POLYMERS.....	25
3.3.1 Process of light absorption	26
3.4 PHOTOAGEING OF PP.....	27
3.4.1 Mechanism of polypropylene photo-oxidation: Radical mechanism.....	27
3.5 CONSEQUENCES OF PHOTO-OXIDATIVE DEGRADATION.....	28
3.5.1 Fissuring.....	28
3.5.2 Influence of processing, irradiation and oxidation parameters	29
3.5.3 Influence of crystallinity	30
4 ACCELERATED WEATHERING TESTS.....	31
4.1 ACCELERATED AGEING DEVICE – SEPAP 12.24.....	31
4.1.1 Components of SEPAP 12.24	32
5 METHODS OF ANALYSIS.....	33
5.1 INFRARED SPECTROSCOPY	33
5.1.1 Fourier transform infrared spectroscopy	34
5.1.1.1 Micro-infrared spectroscopy	35
5.1.1.2 Attenuated total reflection infrared spectroscopy.....	35
5.1.2 Comparison of ATR and FTIR spectroscopy.....	37

II	EXPERIMENTAL	38
6	MATERIAL	39
7	SAMPLES PREPARATION	40
7.1	COMPRESSION-MOULDED SAMPLES	40
7.2	INJECTION-MOULDED SAMPLES	40
8	ACCELERATED PHOTOAGEING.....	42
8.1	COMPRESSION-MOULDED SAMPLES	42
8.2	INJECTION-MOULDED SAMPLES	42
9	ANALYSING METHODS AND DEVICES	43
III	RESULT AND DISCUSSION	44
10	PHOTOCHEMICAL BEHAVIOUR OF FILMS HAVING DIFFERENT THICKNESS.....	45
11	DEGRADATION PROFILE.....	50
12	PROCESSING-INDUCED MORPHOLGY	52
	CONCLUSION	55
	REFERENCES.....	56
	LIST OF SYMBOLS AND SHORTCUTS	61
	LIST OF FIGURES	62
	LIST OF TABLES.....	63

INTRODUCTION

It would be difficult to imagine the modern world without plastics. Today they are an integral part of everyone's life-style, with products varying from commonplace domestic to sophisticated scientific products [Rosato et al., 2004].

Plastics are major materials with many unique applications. They substitute traditional materials such as stone, metals, and wood. The production of plastics however grows faster than that of other materials. The rapid growth of the plastics production is caused by three factors: (1) world population growth, (2) average increase of living standard, and (3) replacement of older materials by plastics [Elias, 2003].

The growth of the plastic industry for over a century has been spectacular evolving into today's routine to sophisticated high performance products. Example of these products include packaging, building, and construction, electrical and electronic appliance, and automotive and aircraft parts [Rosato et al., 2004].

Polyolefins, i.e., the polymers synthesized from olefinic monomers, are the major commercial thermoplastics [White and Choi, 2005]. Isotactic polypropylene (iPP) is one of the most important semicrystalline polymers [Rosato et al., 2004]. This polymer exhibits excellent chemical resistance, low density, relatively high tensile strength and high melting point. From the scientific point of view, PP is interesting because of its polymorphism (α , β and γ crystalline phases) [Čermák et al, 2005]. Polypropylene is one of two largest thermoplastics in volume and it is fabricated into filaments, films, and moulded parts [White and Choi, 2005].

The increased outdoor use of plastics has created a need for a better understanding of the effect of the environment on plastics materials [Shan, 1998]. The changes that can occur in a material with photo-ageing can affect its application, performance, and lifetime; therefore, a study of this effect is very important.

Polypropylene (PP) is unstable in the presence of oxidation conditions and UV radiation. Without the stabilizers, PP in a form of the films, the plates or in the fibers exposed to the common utilization outside conditions degrades readily and loses its mechanical properties [Grossetete, 2001].

The aim of this master thesis was to assess the effects of individual physical factors in photodegradation of polypropylene. The specimens were prepared via compression

moulding and injection moulding. Subsequently, the specimens with various processing history and shapes were exposed to UV-light in accelerated ageing device. The extent of photooxidation was measured using FTIR spectroscopy, ATR spectroscopy and micro-infrared spectroscopy.

I. STATE-OF-THE-ART

1 POLYPROPYLENE

The first polymer of propylene was already prepared in 1869 by Marcelin Berthelot. A product of a propylene and sulphuric acid reaction was at the time a sticky precipitate [Lapčík and Raab, 2004]. Thus, PP with his asymmetric carbon atoms was known as a rubbery waxy non-crystalline material [White and Choi, 2005]. No utilization was found for this substance. Therefore, modern history of PP started in 1952 [Lapčík and Raab, 2004].

Giulio Natta was a research assistant in Ziegler's Mülheim laboratory and became very familiar with his new system of linear low-pressure polyethylene synthesis occurring through catalysis by aluminium alkyls with an addition of titanium co-catalysts. He was aware that Ziegler had tried to polymerise propylene but had not considered it successful. In 1953–1954, Ziegler sold parts of his catalysts to various industrial companies and one of them – Montecatini Company from Italy – made arrangements with Prof. Giulio Natta and his co-workers to apply these catalysts to a range of monomers. The first crystalline PP was synthesized by Natta et al. in March 1954. It has a density of 0.91 g/cm^3 and crystalline melting temperature of about $165 \text{ }^\circ\text{C}$ [White and Choi, 2005].

The development of catalysts for PP polymerisation in the 1950's made the production of stereospecific PP possible and led to the rapid growth rate of PP that is still occurring today [Maier and Calafut, 1998]. Isotactic PP is produced by many world prominent companies either in a pure form or with various modifiers. Among the most widely known foreign producers of PP in the Czech Republic belong: Slovnaft (TATREN), Vestolen (VESTOLEN), BASF (NOVOLEN), Hoechst (HOSTALEN), Borealis, PCD (DAPLEN), DMS (STAMYLAN P), Elf Atochem (APPRYL), Solvay (ELTEX), Montell (MOPLEN), Hungarian TIPPLEN, American companies Exxon (SCORENE), Dow, Amoco and others. Czech Chemopetrol produces iPP under the name MOSTEN. Technology is based on Amoco license [Lapčík and Raab, 2004].

1.1 Polymerization reaction

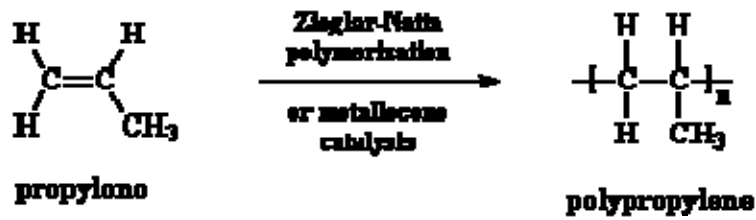


Figure 1. Polymerisation reactions of propylene units [www 1]

PP is prepared by polymerizing propylene, a gaseous by-product of petroleum refining, in the presence of a catalyst under the carefully controlled heat and pressure. PP is an unsaturated hydrocarbon, containing only carbon and hydrogen atoms. In the polymerization reaction, many propylene molecules are joined together to form one large molecule of PP. A long, linear polymer chain of carbon atoms is formed, with methyl (CH₃) groups attached to every other carbon atom of the chain as shown in Figure 1. Thousands of propylene molecules can be added sequentially until the chain reaction is terminated [Maier and Calafut, 1998].

1.2 Structure of polypropylene

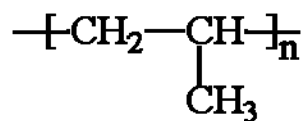
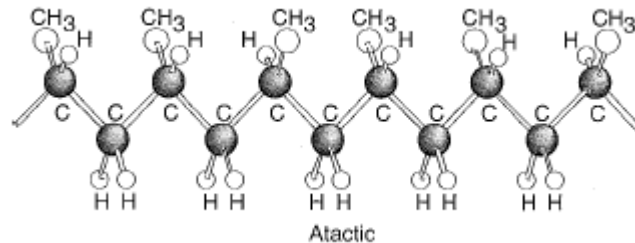


Figure 2. One mer unit of the propylene macromolecular chain [www 1]

The basic building unit is a repeating unit of propylene. The arrangement of a monomer propylene unit is relatively exactly determined by the valence angles between the carbon atoms. The propylene units are asymmetric, thus they may compose the macromolecule in different ways. According to this way there are three types of PP – isotactic, syndiotactic

and atactic [Lapčik and Raab, 2004]. Each kind is determined by the orientation of the pendant methyl groups attached to alternate carbon atoms [Maier and Calafut, 1998].

1.2.1 Atactic polypropylene



*Figure 3. Atactic polypropylene structure
[Osswald and Menges, 2003]*

Generally atactic polymers are characterized by their tacky, amorphous behaviour and low molecular weights. Atactic portion provide the same effect as plasticizer, by reducing the crystallinity of the PP. A small amount of atactic polymers in the final polymer can be used to improve certain mechanical properties. This provides properties to the final polymer such as improved low temperature performance, elongation, processability and optical properties (transparency), but sacrifices flexural modulus or stiffness, and long-term heat ageing units [Mark and Alger, 1989].

Configuration of atactic polypropylene (aPP) is randomly distributed in the repeat units. The structure is irregular, the polymer is weakly rubbery compared with isotactic polypropylene, which is hard and stiff. Atactic polypropylene cannot crystallize. Macromolecular chain of atactic PP is shown in Figure 3 [Mark and Alger, 1989; Lapčik and Raab, 2004].

1.2.2 Syndiotactic polypropylene

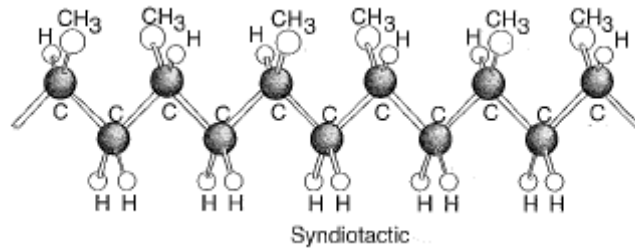


Figure 4. Syndiotactic polypropylene structure
[Osswald and Menges, 2003]

Syndiotactic polypropylene (sPP) is defined by methyl groups arranged alternatively on both side of the zigzag chain, and it is obtained by alternative addition of the two stereoisomeric configuration form of propylene monomer [Monasse and Haudin, 1995]. Syndiotactic polypropylene structure is presented in Figure 4. Sequence for each syndiotactic unit has setting up a helix with two syndiotactic units per turn with the identity period 0.74 nm [Čermák, 2005].

Table 1. The unit cell parameters of sPP crystalline forms [White and Choi, 2005]

PP	Crystalline form	Chain conformation	Unit cells (Length: nm)
SYNDIOTACTIC	Form I [Lotz et al.]	S(2 ₁) ₂ helix: (T ₂ G ₂) ₂	Orthorombic (a = 1.45, b = 1.12, c = 0.74, α = β = γ = 90°)
	Form II [Corradini et al., 1967]	S(2 ₁) ₂ helix: (T ₂ G ₂) ₂	Orthorombic (a = 1.45, b = 0.56, c = 0.74)
	Form III [Chatani et al., 1990]	Planar zig-zag: (TTT)	Orthorombic (a = 0.522, b = 1.117, c = 0.506)
	Form IV [Chatani et al., 1991]	(T ₆ G ₂ T ₂ G ₂)	Triclinic (a = 0.572, b = 0.764, c = 1.160, α = 73.1°, β = 88.8°, γ = 112.0°)

The stable structure of sPP possesses a unit cell which includes 2 left - and 2 right - handed helices in a regular alternation along both the a and the b axis [Čermák, 2005].

A stable modification characterized by a chain in the $s(2_1)2$ helical conformation can be packed in different crystalline cells (named Form I and II) depending on the degree of stereoregularity and the mechanical and thermal history of the sample. A different form (Form III) can be obtained by stretching the compression-moulded samples and it is characterized by a chain in zigzag planar conformation. Form IV was obtained by Chatani et al. [1991] by exposing fibre specimens in the zigzag conformation to organic solvents, such as benzene. It is characterized by helices in a $(T_6G_2T_2G_2)_n$ conformation, packed in triclinic cell [Guadagno et al., 1999].

As mentioned before, highly stereoregular sPP samples have been made available mainly because of the new metallocene-catalyst technology [Wang et al., 2001], commercial production is not possible with ZN catalysts [Graves, 1994]. Syndiotactic PP has finally found the exercise in adhesive, caulks, and cable-filling compounds [Mark and Alger, 1989]. The unit cell parameters of sPP crystalline forms are listed in Table 1.

1.2.3 Isotactic polypropylene

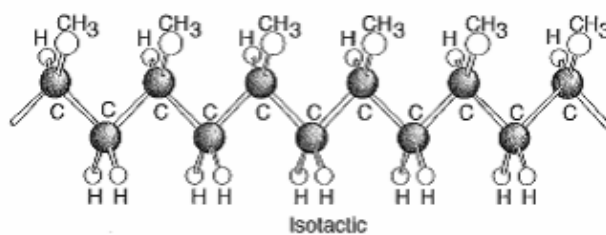


*Figure 5. Isotactic polypropylene structure
[Osswald and Menges, 2003]*

The most common commercial form is iPP. In this modification pendant methyl groups are all in the same configuration i.e. are on the same side of the polymer chain as shown in Figure 5. Due to this regular, repeating arrangement, iPP has a high degree of crystallinity [Maier and Calafut, 1998]. Isotactic PP structure is one of the most complex commercially developed polymeric materials, because it has a number of crystal modifications [Al-Raheil et al., 1998].

1.3 Polymorphism of isotactic polypropylene

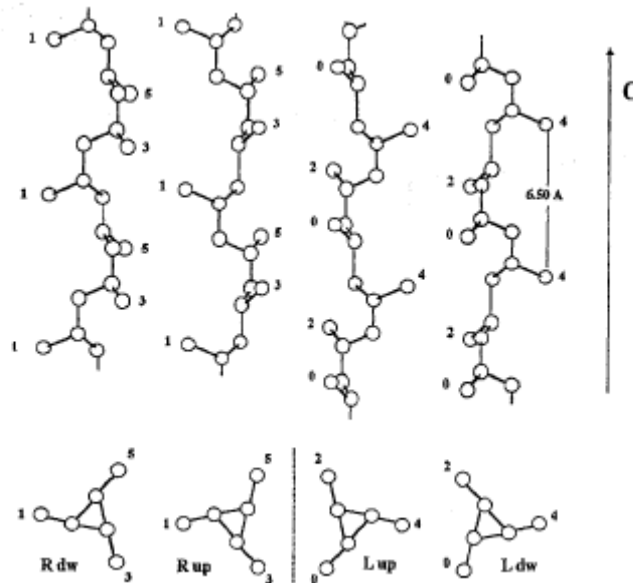


Figure 6. Four possible arrangements of the *iPP* chain in a crystal lattice [Karger-Kocsis, 1999]

The chains of the *iPP* form 3_1 -helix conformation in crystalline regions. The helix is either left - or right - handed with *up* or *down* position of pendant methyl groups (see Figure 6) [Čermák, 2005]. The identity period is 0.65 nm long [Lapčík and Raab, 2004]. Depending on crystallization conditions, such as, temperature, cooling rate, and pressure, the helices can be packed into three different crystalline forms denoted α , β , γ which differ in crystal lattice and, consequently, in properties. Each of these forms manifests specific diffraction spectra as shown in Figure 7 [Čermák, 2005].

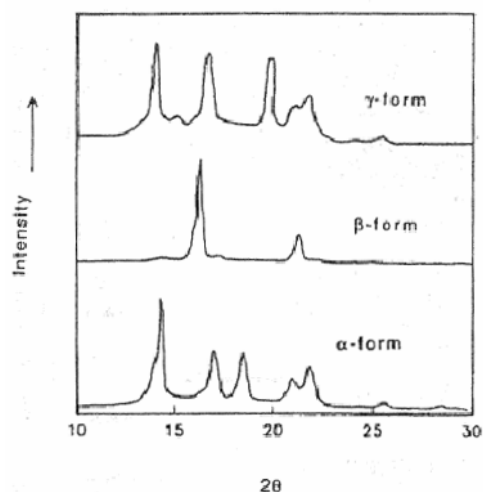


Figure 7. The diffraction spectra of crystalline α , β and γ forms of iPP [Obadal, 2002]

In addition to crystalline forms, mesomorphic smectic modification was also identified in iPP [Čermák, 2005]. Morphologies of the α - and β - forms are usually spherulitic, in the case of melt crystallization [Al-Raheil et al., 1998].

Table 2. The unit cell parameters of iPP crystalline forms [White and Choi, 2005]

PP	Crystalline form	Chain conformation	Unit cells (Length: nm)
ISOTACTIC	α -form [Natta and Corradini, 1959]	3_1 helix:	Monoclinic ($a = 0.665$, $b = 2.096$, $c = 0.650$, $\beta = 99.3^\circ$, $\alpha = \gamma = 90^\circ$)
	β -form [Karger-Kocsis, 1999]	3_1 helix:	Trigonal ($a = b = 1.101$ nm, $c = 0.650$ nm)
	γ -form [Brückner and Meille, 1989]	3_1 helix:	Orthorombic ($a = 0.854$, $b = 0.993$, $c = 4.241$, $\alpha = \beta = \gamma = 90^\circ$)
	Mesomorph (smectic) [Natta et al., 1959]	3_1 helix:	----

1.3.1 α -form

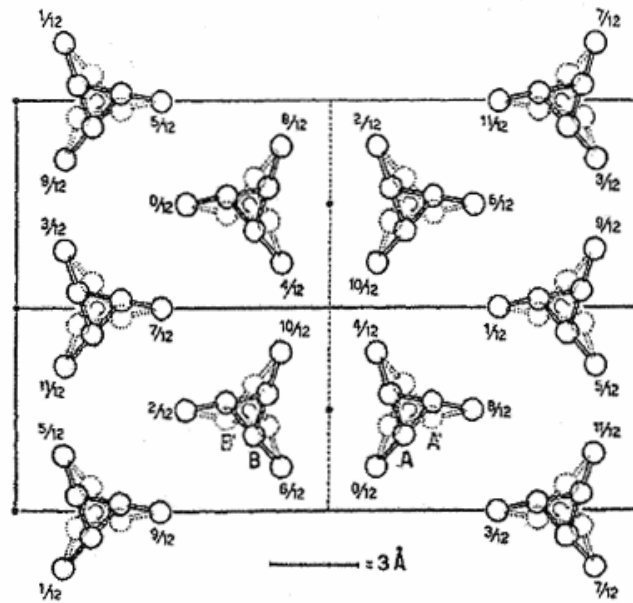


Figure 8. Crystal structure of α -form of iPP
[Karger-Kocsis, 1999]

Commercial iPP grades have crystallized mostly in α -modification under the usual thermal conditions with only sporadic occurrence of β -modification [Al-Raheil et al., 1998]. The monoclinic α -structure is thermodynamically the most stable form of all crystalline modification [Zheng et al., 2004]. It has a monoclinic unit cell [White and Choi, 2005]. The unit cell contains two left- and two right-handed helices. The crystal structure of α -form of iPP is given in Figure 8. The unit cell parameters of α -form are listed in Table 2. The melting temperature of α -monoclinic form ranges from 165 to 170 °C, whereas the most reliable value of the equilibrium melting point of the α -form is ranging between 185 °C and 209 °C [Cheng, 1995; Obadal, 2002]. The crystallographic density has been determined 0.938 g/cm³ [Obadal, 2002].

The crystal structure produces positive, negative, and mixed birefringence. Negative birefringence results from spherulites in which radial lamellas are dominant, while positive birefringence is due to spherulites with predominantly tangential lamellas. It has been recognized that this lamellar branching is characterized by a constant angle between tangential and radial lamellas [Karger-Kocsis, 1999]. Khoury has determined value of angle branching about 80° [Obadal, 2002].

Both negatively and positively birefringent spherulites form a Maltese cross pattern under crossed polarizers. In spherulites with mixed birefringence, neither tangential nor radial lamellas are predominant, and a distinct Maltese cross is not formed. The birefringence changes from positive to negative with increasing crystallization temperature, as the tangential lamellas undergo premelting [Philips and Wolkowicz, 1996].

1.3.2 β -form

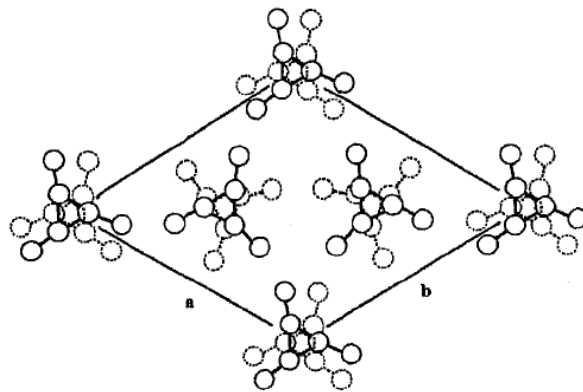


Figure 9. The trigonal unit cell of β -form of iPP [Addink and Bientema, 1961]

The β -crystalline form was first identified in 1959-1960 [White and Choi, 2005]. Under normal melt-crystallization, the β -phase of iPP occurs only sporadically among the predominant α -phase. It is believed that acquiring more β -phase crystal is possible under special conditions, such as quenching the melt to a certain temperature range, directional crystallization in a temperature gradient field, shear-induced crystallization [Zheng, 2004]. β -crystalline form can also be induced by a range of nucleating agents [White and Choi, 2005]. It has been proved that regardless of whether nucleating agents are present or not, high content of β -phase crystal can only be obtained within a limited range of crystallization temperature. Recently, a new experimental phenomenon has been reported, that the β -crystal of the neat PP occurred after vibration plastication in a vibration internal mixer [Zheng, 2004].

The β -form has a trigonal unit cell as shown in Figure 9. There has been much controversy over the unit cell. Keith et al. [1959] proposed the unit cell of β -form to have hexagonal form of $a = 1.274$, $c = 0.635$, $\gamma = 120^\circ$ and $\alpha = \beta = 90^\circ$, but it has been verified by Varga [2002] that the crystal arrangement of the β -form is trigonal. The crystal parameters of

trigonal unit cell are listed in Table 2. The β -form consists of the same 3_1 helices [White and Choi, 2005]. The β -form is metastable [Zheng, 2004]. The crystallographic density has been determined 0.92 g/cm^3 [Obadal, 2002]. The melting temperature of β -phase is in range of $150\text{-}153 \text{ }^\circ\text{C}$. The β -form spherulites are characterized by strong negative birefringence. Padden and Keith [1959] have denoted two types of β spherulites. The spherulites characterized by strong negative birefringence that are formed below $128 \text{ }^\circ\text{C}$ are denoted as negative radial spherulites. The seconds formed in a temperature range $128\text{-}135 \text{ }^\circ\text{C}$ are specified as negative annular spherulites.

The spherulites of β -phase recrystallized into α -modification ($\beta\alpha$ recrystallization) when slowly heated [Baran, 2001].

Some properties of β -iPP differ significantly from those of α -iPP. In comparison with α -iPP, β -iPP possesses lower crystal density, melting temperature and fusion enthalpy, but a similar glass transition. The chemical resistance of β -iPP seems to be lower than that of α -iPP [Jacoby et al., 1986]. β -iPP compared with α -iPP has a lower E-modulus and yield stress, but higher ultimate tensile strength and strain [Varga, 1995]. The impact strength and toughness of β -iPP exceed those of α -iPP [Karger-Kocsis and Varga, 1996].

1.3.3 γ -form

The crystalline γ -form was first observed by Addink and Beintema [1961] and has been subjected to extensive study since that time. As with the β -phase, there was much controversy over the unit cell. Various unit cells have been also proposed by Turner-Jones et al. [1964], Morrow and Newman [1968], and Brückner and Meille [1989]. The view of the latter authors is now generally supported. They proposed an orthorhombic unit cell. The crystallography parameters are listed in Table 2. In the unit cell of the γ -form macromolecules co-exist with non-parallel chain axes, which form an angle of 81° to each other [White and Choi, 2005].

The γ -modification may form in low molecular weight iPP or in samples crystallized under high pressure [Al-Raheil et al., 1998]. Other procedure is crystallization from melt of high molecular weight stereoblock copolymer with small amounts of ethylene or but-1-ene [Phillips and Mezghani, 1996]. The α -form is present at atmospheric pressure; as the pressure is increased, the γ -form begins to co-exist with the α -form until it becomes dominant at a pressure of 200 MPa [Kressler, 1999].

1.3.4 Smectic form

It is possible to prepare a smectic form by quenching thin sheets of iPP from the melt into the ice water [Phillips and Mezghani, 1996]. The smectic structure is less organized than the previous structures; however there are small areas with specific level of arrangement [Natta and Corradini, 1960]. The density of smectic form has been reported by Natta [1959] as 0.88 g/cm^3 [Phillips and Mezghani, 1996].

1.4 Properties of polypropylene

Commercial PP is 90–95% isotactic and has a number average molecular weight of 40 000–60 000 with a polydispersity of 6–12. The crystalline regions have a density of 0.94 g/cm^3 and the amorphous regions have a density of 0.85 g/cm^3 , so that overall, PP has a density about 0.90 g/cm^3 with a crystallinity of about 50%. PP melts may be quenched to give an amorphous polymer. The maximum T_m value is $165 \text{ }^\circ\text{C}$ with narrow (about $5 \text{ }^\circ\text{C}$) melting range, so that PP softens at a considerably higher temperature than polyethylene (PE). Its major amorphous transition is at about $0 \text{ }^\circ\text{C}$ so that the polymer embrittles markedly on cooling [Mark and Alger, 1989].

PP is stiffer than PE, having a tensile modulus of 1000–1300 MPa and a tensile strength of 25–35 MPa. Its elongation at break is 50–300% and its impact strength (Izod) is 0.3–4.3 J. PP is highly solvent resistant and environmental stress cracking resistant. It has very high electrical resistivity. However, the presence of a tertiary carbon on each repeated unit makes it very susceptible to oxidative degradation. Although usually opaque, thin film, especially if biaxially oriented, may show a sparkling degree of clarity. Uniaxially oriented film may be readily split in the direction of orientation to give tape, twine or fibres [Mark and Alger, 1989].

As a plastic material PP is mainly used as an injection-moulded material [Mark and Alger, 1989].

1.5 Morphology associated with processing

It is widely recognized that the morphology of plastics articles strongly depends on processing history. While the moulding polymer is affected by various thermal, mechanical and flow conditions resulting in differences of crystallinity, orientation, and shape and size

of supermolecular aggregates [Čermák, 2005]. The processing of a linear-chain polymer that is glassy or partially crystalline at use temperature requires heating to soften pieces or sheets of the material to be fabricated. Either as or after the object is formed, it is subjected to cooling. In thick samples, a temperature gradient can exist during the cooling phase, causing the outer portion to cool more rapidly than the innermost parts [Woodward, 1995]. The structure of injection-moulded polymers differs from the morphology of compression-moulded polymers. Thus, the difference in a crystal structure causes different, photochemical behaviour during photo-degradation.

1.5.1 Skin-Core and related morphologies

1.5.1.1 Impact of injection moulding on morphology of polymers

Injection-moulded specimens possess different morphologies at the sample surface (the skin) and in the interior (the core), or a trilayer structure consisting of a skin, an intermediate region and a core [Woodward, 1995]. Studies on injection-moulded PP have shown that at least two regions are discernible through the wall thickness [Čermák, 2005]. The skin-core morphology, actually, displays a strong structural heterogeneity through the specimen thickness, and a complicated profile of degradation can be expected. This structural development consequently affects specimen degradability [Obadal et al., 2005]. The injection of a polymer melt into a mould by the application of pressure causes chains to assume elongated conformations in the direction of applied stress. [Woodward, 1995]. If the surface of the mould is cold and the sample is thin, solidification will occur quickly, freezing in some or all of the chain orientation throughout the sample [Woodward, 1995]. If the surface of the mould is cold but the sample is thick, cooling of the polymer in the interior is slower than near the surface, and morphological differences will be observed due to a return to less elongated conformations of the interior chains prior to solidification. The center portion of thick samples (the core) will contain non-deformed spherulites and the surface (the skin) will consist of highly oriented chains [Woodward, 1995].

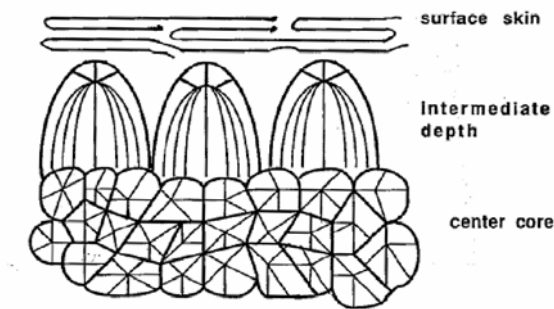


Figure 10. Structure of injection-moulded sample skin-intermediate-core [Woodward, 1995]

For some samples, the spherulites in a region between the skin and the core have conical shapes due to thermal gradients that occur during their formation. The skin-intermediate-core morphology has been observed for PE, polyoxymethylene and iPP. A drawing depicting skin-intermediate-core morphology is given in Figure 10 [Woodward, 1995].

1.5.1.2 Impact of compression moulding on morphology of polymers

During compression moulding pressure is applied to force the material into contact with all mould areas, and heat and pressure are maintained until the moulding material is solidified. Material is not subjected to the pressure to induce flow and because the pressure facilitating flow is not applied before cooling, thus the molecular chains in the upper layer are not oriented.

The supermolecular architecture through the sample of compression-moulded polymer consists of two regions. For upper layer cooling can lead to form conical spherulites. The innermost layer of specimen contains non-deformed spherulites.

2 DEGRADATION

The increased outdoor use of plastics has created a need for a better understanding of the effect of the environment on plastics materials. The environmental factors have significant detrimental effect on appearance and properties. The severity of the damage depends largely on such factors as the nature of environment, geographic location, type of polymeric material, and duration of exposure. The effect can be anywhere from a mere loss of colour or a slight crazing and cracking to a complete breakdown of the polymer structure. Any attempt to design plastics parts without a clear understanding of the degradation mechanisms induced by environment would result in a premature failure of the product. The major environmental factors that seriously affect plastics are [Shan, 1998]:

- Solar radiations-UV, IR, X-rays
- Microorganism, bacteria, and fungus
- High humidity
- Ozone and oxygen
- Water: vapour, liquids, or solid
- Thermal energy
- Pollution: industrial chemicals [Shan, 1998]

Resistance against the influence of environment on polymeric materials depends on their chemist, molecular structure, amount and type of additives, presence of impurities, mode of processing and processing conditions and effecting environment. Ageing of plastics is defined as a complex of irreversible changes of material characteristics caused by chemical, physicochemical and physical processes leading to undesirable non-reversible changes of the polymer features. Deterioration of polymeric materials is effected by light, weather conditions, temperature, ozone, oxygen, chemical attack or mechanical stress. Degradation is defined as a complex of destructive reactions of polymers that include processes leading to splitting of macromolecule to smaller elements. There are several types of degradation processes: [Doležel, 1981].

- Thermic degradation is caused by thermic stress without presence of oxygen.
- Thermo-oxidative degradation is thermic process occurring in presence of oxygen.

- Photodegradation is destruction caused by the light.
- Photo-oxidative degradation is similar to the photodegradation but in presence of oxygen.
- Biological degradation.
- Mechanodegradation is caused by mechanical stress.
- Chemodegradation is degradation influence by the chemicals.
- Ionizing degradation [Doležel, 1981].

Table 3. Relative weather resistances of unmodified thermoplastics [Shan, 1998].

Polymer	Resistance
Acrylics	High
PTFE and other fluorocarbons	High
Polycarbonate	Medium
Thermoplastics polyester	Medium
Nylons	Medium
Polyurethanes	Medium
Rigid PVC	Medium
Flexible PVC	Low
ABS	Low
Polyethylene	Low
Polysulfone	Low
Polystyrene	Low
Polypropylene	Low

3 PHOTODEGRADATION

3.1 Light source

In practical applications of polymers the sun is the most important light source. The spectrum of sunlight penetrating to the earth's surface ranges from about 290 to 3000 nm. The spectral distribution depends on atmospheric conditions and the latitude. Somewhat less than 10% of the sunlight at the earth's surface is UV-light, about 50% is visible and about 40% is IR light [Schnabel, 1981].

3.2 Electromagnetic radiation

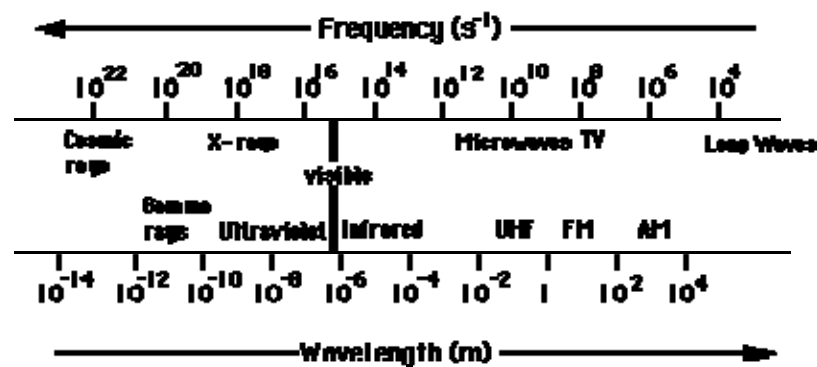


Figure 11. Electromagnetic spectrum [www 2]

Electromagnetic radiation is classified into types according to the frequency of the wave. In order of increasing frequency these types include: direct currents, induction heating, radio waves, microwaves, terahertz radiation, infrared radiation, visible light, ultraviolet radiation, X-rays, γ -rays and cosmic photons [www 3]. A portion of the electromagnetic spectrum is shown in Figure 11, along with the names associated with various regions of the electromagnetic spectrum [www 2].

Electromagnetic waves travel at the speed of light (c), and are characterized by frequency (ν) or wavelength (λ) and amplitude. The frequency and wavelength are related by the equation [www 2]:

$$c = \nu * \lambda \text{ [m/s]}. \quad (3.2.1)$$

The relationship between energy and frequency is given by Planck's Law. It describes the amount of absorbed energy [www 4]:

$$E = h * \nu [J], \quad (3.2.2)$$

where E is energy emitted by light photon of radiation and h is Planck's constant [6.626x10⁻³⁴J.s] [www 4].

Planck's Law can be also expressed as [www 2]:

$$E = \frac{h * c}{\lambda} [J]. \quad (3.2.3)$$

Electromagnetic radiation carries energy and momentum which may be imparted when it interacts with matter [www 3]. Polymers can absorb UV-light, X-rays, γ -rays and cosmic radiation [Hagen, 1977].

3.3 Impact of ultraviolet radiation on polymers

Light-induced polymer degradation concerns the physical and chemical changes caused by interaction of polymers with UV or visible light. Therefore, photoreactions are usually induced when organic polymers are subjected to outdoor exposure [Schnabel, 1981, Hagen, 1977]. The photo-oxidation process is conditioned by absorbing of radiation energy to polymer and absorbed energy quantum must be larger or at least equal to the bonds dissociation energy [Hagen, 1977]. The resulting chemical processes may lead to severe properties deteriorations, such as the chains scission, crosslinking and when it occurs in presence of oxygen to activation of oxidation processes.

The polymers exposed to UV-light have a tendency to oxidize mainly because of presence of impurities called the chromophores which can be contained in material matrix. These constituents can absorb UV-light. Photochemically important chromophores absorb in the UV range (i.e. at wavelengths below 400 nm). Light absorption in a molecule means a specific reaction of certain chromophoric group with a photon of given energy. The remainder of the molecule remains unaffected during the absorption act. The existence of chromophores in the macromolecules (or in additives) is a prerequisite for the initiation of photochemical reactions. It explains, in most cases, the instability of polymers, which, according to their chemical constitution, should be resistant to solar radiation [Schnabel, 1981].

Light is absorbed statistically by the chromophores in a system. Thus, we know there is a probability for the absorption of a certain photon by a certain chromophores, but we do not

know when it happens. In a light absorbing homopolymer there is equal probability for the absorption of a photon by all base units. Chemical reactions occurring subsequent to light absorption can be initiated at any place in the macromolecule [Schnabel, 1981].

Saturated compounds possessing bonds such as C-C, C-H, O-H and C-Cl absorb light at wavelength $\lambda \leq 200$ nm. Carbonyl groups and conjugated C=C bonds absorb above $\lambda = 200$ nm and have absorption maxima between 200 and 300 nm [Schnabel, 1981].

In general, photoreactions in commercial polymers are harmful. They cause embrittlement and colour changes [Schnabel, 1981].

3.3.1 Process of light absorption

The chance of an absorbed photon to induce a chemical change in the molecule depends principally on the photophysical processes following the absorption act [Schnabel, 1981].

The absorption of a photon can proceed either as $S_0 + h\nu \rightarrow S_1$ or as $S_0 + h\nu \rightarrow T_1$. The extinction coefficients differ appreciably: $\epsilon(S_0 \rightarrow S_1) \gg \epsilon(S_0 \rightarrow T_1)$. Therefore $S_0 \rightarrow T_1$ processes (designated as “forbidden”) are negligible with respect to photochemical changes. Commonly, owing to their relatively long lifetimes, chemical reactions originate from S_1 or T_1 states [Schnabel, 1981].

After light quantum is absorbed molecule comes from the ground state S_0 to the excited state S_1 : $S_0 + h\nu \rightarrow S_1$. A molecule in its excited singlet-state, S_1 , can relax by various competing pathways. It can undergo “non-radiative relaxation” in which the excitation energy is dissipated as vibrations or heat. Relaxation of an S_1 state can also occur through emission of photon. It results in fluorescence (emission): $S_1 \rightarrow S_0 + h\nu'$. Fluorescence occurs when a molecule relaxes to its ground state after being electronically excited [www 5].

Excited molecules can also relax via conversion to a triplet state T_1 . The triplet state may subsequently relax via phosphorescence: [www 5] $S_0 + h\nu \rightarrow S_1 \rightarrow T_1 \rightarrow S_0 + h\nu'$ [www 6]. Phosphorescence is a process in which energy absorbed by a substance release relatively slowly in the form of light [www 6].

Radiative and radiationless deactivation processes of S_1 states occurs rapidly. Generally fluorescence occurs much faster than phosphorescence [Schnabel, 1981].

3.4 Photoageing of PP

Table 4. Factors affecting resistance of material to photodegradation [Grossetete, 2001]

UV + TEMPRERATURE + OXYGEN ↓ PHOTODEGRADATION		
<i>Factors affecting photochemical behaviour of material</i>		
CHROMOPHORES	CHEMICAL STRUCTURE	PHYSICAL STRUCTURE
<i>Impurities</i>	<i>Repeating units</i>	<i>Crystallinity</i>
<i>Processing</i>	<i>Molecular weight</i>	<i>Orientation</i>
	<i>Tacticity</i>	<i>Crystal size</i>

Ageing of a polymer material within its utilization induces a deterioration of its mechanical properties. This oxidative ageing depends on many factors such as environment conditions (UV, temperature, pollution); thermo-mechanical history (processing of a sample) and material structure [Grossetete, 2001].

3.4.1 Mechanism of polypropylene photo-oxidation: Radical mechanism

Without the stabilizers, PP in a form of the films, the plates or in the fibres exposed to the common utilization outside conditions degrades readily and loses its mechanical properties. The loss of the material properties results from numerous chain breakdowns that then cause the modification of the chemical structure of macromolecules. The formation of numerous oxidation products which are the result of the radical reaction is evident from the polymer analysis. The radical reaction has three main phases which are initiation, propagation, termination [Grossetete, 2001].

In an oxidative reaction the products such as hydroperoxides and ketones are formed. The hydroperoxides are unstable (thermally and photochemically), they are simply decomposed. Ketones are decomposed by incidence of sunlight according to Norrish type reaction I. During the PP photo-oxidation some other photoproducts are detectable. Their presence generally explains a complex structure of an absorption peak in the carbonyl area (between 1900 and 1600 cm^{-1}). The lactones, per lactones, esters or peresters and carboxyl acids are formed as the other products of photo-oxidation of PP [Grossetete, 2001].

3.5 Consequences of photo-oxidative degradation

3.5.1 Fissuring

Fissures develop in polymers which are subjected to outdoor exposure. An apparition of the fissures is related to a process of photo- or thermo- degradation with defined irradiation time and oxidation degree. Most of authors agree with location of fissuring initiation into the amorphous phase of semicrystalline polymers [Grossetete, 2001].

According to Sarwade et al. [1999] an appearance of microfissures on the photo-oxidized surface of polymer results from a chain scission. Free radicals can break away a hydrogen atom from a macromolecular chain and form fragments which occupy larger extent than the original macromolecule. This phenomenon causes stresses and deformations on the polymer surface where the formation of the fissures starts [Grossetete, 2001].

According to Friedrich et al. [1983] photo-degradation causes creation of microzones that are highly disarranged and oxidized. In these areas it is probable a formation of empty microspaces. Migration of instable photoproducts and concentration of the empty microspaces are becoming to be sufficient enough in order to inner initiative stresses cause initiation of material cracking. The material cracking is influenced by temperature parameters, deformation rate (during the applied stress) and material characteristics. It concerns the transformation affecting the macromolecular orientation. Conditions of injection moulding that influence directly a morphology cause creation of different types of nets of fissures [Grossetete, 2001].

- In films fissures are formed according to spherulites rays;

- on a surface of plates they are formed perpendicularly to the direction of injection [Grossetete, 2001].

3.5.2 Influence of processing, irradiation and oxidation parameters

Conditions of processing which affect the physic structure directly and various chromophores in the material play an important role in photo-degradation [Grossetete, 2001].

Oxidation process of polyolefins is controlled mainly by the amount of chromophores which are present in material. However, the physique structure of PP that includes crystallinity, molecular orientation and extent of spherulites affects the photo-oxidation as well. Molecular weight distribution, crystallinity and molecular orientation affect mobility of radicals and control the extension of the termination by recombination [Grossetete, 2001].

The photo-oxidation process essentially depends on an oxygen diffusion. The rate of the oxygen diffusion decreases with increasing crystallinity and orientation of macromolecular chains [Obadal, 2005]. For injection-moulded specimens (thick-walled articles) determination of the degradation level is made more difficult because of the oxygen-diffusion limited effect. If the rate of oxygen consumption exceeds the rate of oxygen permeation, oxidation occurs in the surface layers whereas the core remains virtually unoxidized. This effect is influenced by intrinsic parameters like reactivity of the polymer, presence of chromophoric impurities or physical structure and external factors (i.e. conditions of accelerated ageing or oxygen pressure) [Obadal et al., 2005]. From the scheme of degradation profile depending on the polymer thickness it is perceptible that the oxidation in the surface layers is more apparent than in the inside layers [Grossetete, 2001].

The irradiation conditions affect the stoichiometry and the rates of the formation of oxidation products. Light intensity affects a mechanism of decomposition of hydroperoxides with regard to stoichiometry of the photoproducts. The augmentation of light intensity supports formation of esters and low molecular weight acids. Decreasing of light intensity supports formation of carbonyls (1720 cm^{-1}) and carboxyl acids (1712 cm^{-1}). This stoichiometry modification can be explain by accumulation of hydroperoxides which

either decompose to form mostly acids or react with carbonyls to form esters [Grossetete, 2001].

3.5.3 Influence of crystallinity

Amorphous and crystalline phases affect diffusion of free radicals or oxygen into a polymer. In an amorphous part of semicrystalline polymer oxygen molecules react with free radicals from the beginning of their formation whereas they penetrate harder into a crystalline phase. The radical formed in the crystalline part must diffuse on the crystallite surface to react with oxygen [Grossetete, 2001].

Photo-oxidation of polyolefins induces changes of a crystallinity degree. It has been proved that the crystallinity degree increases during photo-oxidation. It has been attributed to a recrystallization that follows the chain scission. A recrystallization evokes an apparition of small lamellas which are formed at the beginning of ageing process [Grossetete, 2001]. But it is not sufficient to explain an increasing of density during irradiation. Photoproducts such as acids and hydroperoxides aggregate in a polymer matrix, thereby the amount of oxygen increases. As the photo-oxidation time increases a number of photoproducts increases as well; so there is an irregularity of the PP macromolecular chains which crystallize harder. An augmentation of density during irradiation is, thus, influenced by recrystallisation when small lamellas which are formed by branching appear; and by augmentation of oxygen amount. Oxidation products accumulate in a polymer [Grossetete, 2001].

4 ACCELERATED WEATHERING TESTS

Most data on the ageing of plastics are acquired through accelerated tests and actual outdoor exposure. The latter is a time-consuming method; accelerated tests are often used to expedite screening the sample with various combinations of additive levels and ratios. A variety of light sources are used to simulate the natural sunlight. The artificial light sources include carbon arc lamps, xenon arc lamps, fluorescent sun lamps, and mercury lamps. These light sources, except the fluorescent, are capable of generating a much higher light intensity than natural sunlight [Shan, 1998].

4.1 Accelerated ageing device – SEPAP 12.24

The SEPAP 12.24 is a device for performing accelerated tests in order to examine photoageing of polymer materials. The behaviour of the material properties is observed as a function of the duration of exposure [www 7].

The SEPAP 12.24 is the result of extensive studies carried out by the Photochemistry Laboratory at the Blaise Pascal University (Clermont-Ferrand, France) in the field of photoageing mechanisms of polymer materials. Prof. Lemaire from CNEP laboratory (Centre National d’Evaluation de Photoprotection - A centre transferring the results of fundamental research on organic materials ageings) invented SEPAP 12.24 weathering device about 20 years ago. The SEPAP test is based on an ultra photo-oxidation acceleration of polymer materials and was originally designed for testing of thin films (up to 50 μm) [www 8].

This unit makes possible to run accelerated photoageing tests under controlled conditions relevant to natural ageing. It is strongly recommended to follow the chemical evolution of the polymer compounds, either by analyzing the formation of chemical groups occurring during the phototransformation of the matrix and the photooxidation process, or, by analysing the evolution of the stabilizers. This test equipment allows to predict the lifetime of polymer matrices as well as to develop either photostable or photochemically degradable compounds. Thus, a rapid, non-destructive and highly relevant method is implemented to study the complexity of phenomena involved in the photoageing process [www 7].

4.1.1 Components of SEPAP 12.24

The type of radiation used simulates the process of natural photoageing. The four mercury vapour arc lamps with a borosilicate envelop emit intense light in the wavelength range between 290 and 450 nm, thus providing a significant contribution to the accelerated testing. The employed light sources provide a constant radiation level for a period of approx. 4.000 hours as well as a uniform spectral distribution. [www 7].

The precise and air-permeable design of the sample carousel optimises air circulation and thus temperature distribution on the surface of the samples. The rotating movement of the carousel on which the samples are fixed guarantees uniform irradiation on their surfaces.

The SEPAP 12.24 allows for the simultaneous exposure of 24 or 48 samples (depending on size). The temperature probe is in direct contact to one of them. For inserting the samples the carousel is removed from the test chamber and mounted on a pedestal [www 7].



Figure 12. Accelerated ageing device SEPAP 12.12 [www 7]

The temperature is controlled by the microprocessor which regulates the air input and the heaters. The air flow produced by two fans guarantees a homogenous temperature distribution on the sample surface. The Pt (Platinum) temperature sensor (4-wire design) measures the temperature on the surface of the sample. The values are within a range of + 45 °C to + 80 °C, with a ± 2 °C accuracy [www 7].

In the most cases polymer oxidation is evaluated with infrared analysis by screening the C=O value [www 8].

5 METHODS OF ANALYSIS

5.1 Infrared spectroscopy

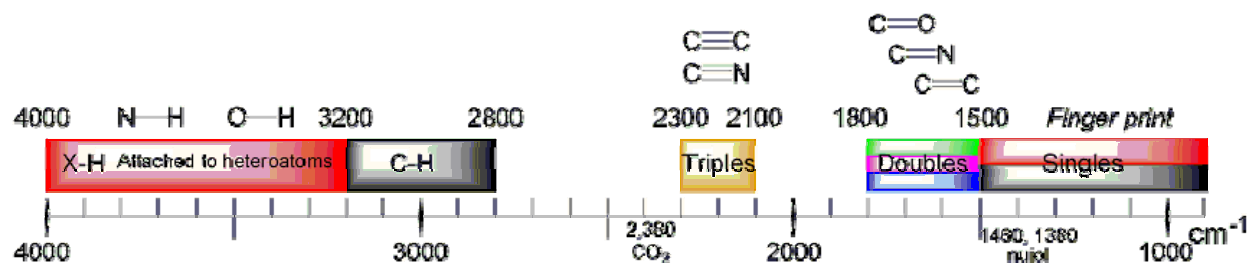


Figure 13. Infrared spectroscopy correlation table [www 9]

Infrared (IR) spectroscopy is subset of spectroscopy that deals with the infrared region of the electromagnetic spectrum [www 9]. IR spectroscopy is very useful for qualitative analysis (identification) of organic compounds because a unique spectrum is produced by every organic substance with peaks corresponding to distinct structural features [www 10].

IR radiation is electromagnetic radiation in the wavelength range 0.78–1000 mm which corresponds to the wave number range 12 800–10 cm⁻¹. The IR portion is usually divided into near- (13000–4000 cm⁻¹), mid- (4000–200 cm⁻¹) and far-IR region (200–10cm⁻¹), whereas most widely used is mid-IR region [www 11] (studying the fundamental vibrations and associated rotational-vibrational structure [www 9]).

A beam of IR light is passed through a sample, and the amount of energy absorbed at each wavelength is recorded [www 9]. In an output IR spectrum energy is plotted as a function of a wavelength.

Energy is usually expressed as a Transmittance (T) or as an Absorbance (A). Energy function on a wavelength is logarithmic, consequently a wave number is often used in the place of a wavelength; a wave number is defined as a reciprocal value of a wavelength; therefore the energy function on a wave number is linear [www 11].

A transmittance is a fraction of light intensities which passed trough a sample (I) to light intensity coming out of a light source (I₀) and it denoted in percents.

$$T = \frac{I}{I_0} [\%] \quad (5.1.1)$$

An absorbance is defined as minus common logarithm of transmittance [www 11].

$$A = -\log T [-] \quad (5.1.2)$$

IR radiation can only be absorbed by bonds within a molecule, if the radiation has exactly the right energy to induce a vibration of the bond. This is the reason why only specific wavelengths are absorbed [www 10].

Radiation is absorbed resulting in a series of peaks in the spectrum, which can then be used to identify the sample. Peaks in the spectrum can be also used for quantitative analysis of some organic compounds. A wavelength of light which has been absorbed is characteristic of the chemical bond. Therefore, the chemical bonds in a molecule can be determined by interpreting an IR absorption spectrum [www 12]. For example, a carbonyl group, C=O, always absorbs infrared light at 1670–1780 cm^{-1} , which causes the carbonyl bond to stretch [www 10].

5.1.1 Fourier transform infrared spectroscopy

It can be applied to a variety of types of spectroscopy including IR spectroscopy. Fourier transform infrared spectroscopy (FTIR) is perhaps the most powerful tool for identifying types of chemical bonds (functional groups) [www 12].

Measurement on the Fourier transform infrared spectrometer (FTIR spectrometer), is based on the spectrum interference principle, thus it monitors interference of the beam of IR light after IR radiation is passed through the sample [www 11]. The amount of energy absorbed at each wavelength is recorded and the spectra are collected [www 9]. FTIR spectrometers use Fourier transform mathematic method to obtain conventional transmission spectrum [www 11]. Fourier transform instrument allows measuring of all wavelengths at once [www 9].

FTIR can be used to identify chemicals from spills, paints, polymers, coatings, drugs, and contaminants. FTIR spectra of pure compounds are generally so unique that they are like a molecular "fingerprint" [www 13].

5.1.1.1 Micro-infrared spectroscopy

Micro-infrared (μ -IR) spectroscopy is an experimental arrangement in which IR spectrometer is coupled with a microscope. This arrangement allows an examination of the degradation profile [Obadal et al., 2005].

5.1.1.2 Attenuated total reflection infrared spectroscopy

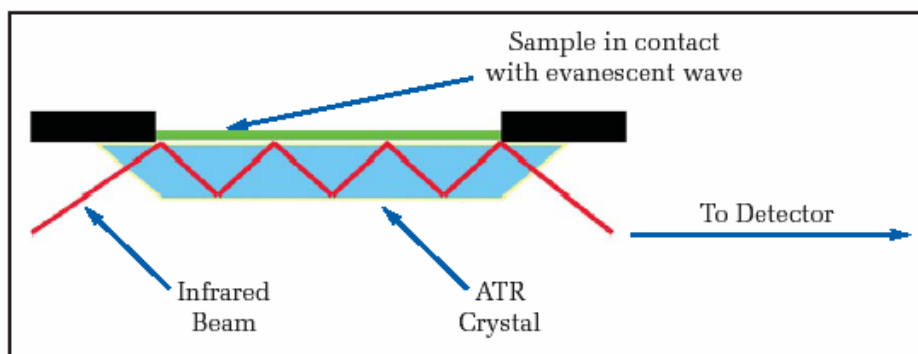


Figure 14. Attenuated total reflection infrared spectroscopy accessory [www 13]

Attenuated Total Reflection (ATR) is a sampling technique used in conjunction with IR spectroscopy which enables samples to be examined directly in a solid or liquid state without further preparation. An ATR accessory operates by measuring changes that occurs in a totally internally reflected IR beam when the beam comes into contact with a sample as indicated in Figure 14 [www 14].

The IR beam is directed onto an optically dense crystal with a high refractive index at a certain angle. This internal reflectance creates an evanescent wave that extends beyond a surface of the crystal into a sample held in contact with the crystal [www 15].

In regions of an IR spectrum where the sample absorbs energy, the evanescent wave will be attenuated or altered. The attenuated energy from each evanescent wave is passed to the IR beam, which then exits the opposite end of the crystal and is passed to the detector in the IR spectrometer [www 15]. The system then generates an IR spectrum [www 14]. The penetration depth into the surface of the sample is in ones of mm [www 11].

The penetration depth (d_p) into the surface of the sample depends on the IR wavelength according to the Harrick equation [Suetaka, 1995]:

$$d_p = 1 / \left[2\pi n_1 \left(\sin^2 \Phi - (n_1 / n_2)^2 \right)^{1/2} \right] \quad (5.1)$$

where d_p is the analysed thickness at the incidence wavelength λ ; n_1 and n_2 are the refractive indexes of the crystal and the sample, respectively; Φ is the incidence angle.

For the technique to be successful the sample must be in direct contact with the ATR crystal, because the evanescent wave only extends beyond the crystal 0.5 μm –5 μm [www 14].

The refractive index of the crystal must be significantly greater than that of the sample or else internal reflectance will not occur – the light will be transmitted rather than internally reflected in the crystal [www 14].

Typically, ATR crystals have refractive index values between 2.38 and 4.01 at 2000 cm^{-1} . It is safe to assume that the majority of solids and liquids have much lower refractive indices [www 14].

ATR design is commonly horizontal in which a sample is clamped against a horizontal face of the crystal. The crystal is a parallel – sided plate, typically about 5 cm by 1 cm, with the upper surface exposed (see Figure 14). Number of reflections at each surface of the crystal is usually between five and ten, depending on the length and thickness of the crystal and the angle of incidence [www 14].

There are three types of ATR crystal materials – Zinc Selenide, Germanium and Diamond.

Zinc Selenide (ZnSe) and Germanium are by far the most common used. ZnSe is relatively low cost ATR crystal material and is ideal for analysing liquids and non abrasive pastes and gels. But the ZnSe scratches quite easily and there is a problem with a working in the pH range 5-9. Germanium has a much better working pH range and can be used to analyse weak acids and alkalis [www 14].

In the case of a solid sample, generally, they are best analysed with diamond crystal material. It is preferred because for its durability and robustness [www 14]. The solid sample is pressed into direct contact with the crystal. The evanescent wave into the solid sample is improved with a more intimate contact [www 15]. The original purchase cost is obviously higher than that of other crystal materials available, but over the instrument's lifetime replacement costs should be minimal. The same cannot be said of Zinc Selenide or Germanium, both of which can scratch and break with improper use [www 14].

5.1.2 Comparison of ATR and FTIR spectroscopy

The optics involved in ATR is quite different from that used in the transmission experiment. As a result, the IR spectrum of a sample obtained by ATR exhibits some significant differences when compared to its transmission counterpart [Nunn and Nishikida, 2003].

Some of these differences are desirable and have been used to considerable advantage. An example of an advantage of ATR is that it is sensitive to the surface of the sample. As a result, the technique has found utility in the characterization of coatings and the identification of surface contaminants [Nunn and Nishikida, 2003].

Less desirable characteristic of ATR are its distortion of relative intensities of bands and the introduction of a shift to lower frequencies. Therefore, these distortions create problems when comparing spectra obtained by ATR and transmission, but the Advanced ATR correction algorithm corrects for band intensity distortion and peak shifts [Nunn and Nishikida, 2003].

II. EXPERIMENTAL

6 MATERIAL

The basic material used throughout this study was isotactic PP Mosten 58 412 manufactured by Chemopetrol Litvínov a.s., the Czech Republic. This polymer is intended for preparing uniaxially oriented tapes and fibres.

Isotactic PP Mosten 58 412 is characterized by a melt flow index of 3 g/10min (2.16 kg, 230 °C, ISO 1133), a weigh-average molecular weigh approx. 320 000 (GPC) and an isotacticity index of 98% (ISO 9113). The material contained a standard stabilization package based on phenol-phosphite stabilization including Irganox 1010, Irganox 1076 and Irgafos 168 produce by Ciba Specialty Chemicals Inc., Basel, Switzerland.

7 SAMPLES PREPARATION

According to the mode of processing two types of samples were prepared. The processing methods – compression-moulding and injection-moulding – were applied.

7.1 Compression-moulded samples

From polymer pellets films with thickness of approx. 80, 180, 400, 500 and 1000 μm was compression-moulded. After 6-min pressing at 210°C each film was cooled at 60 °C for 8 min. From each compression-moulded film, rectangular specimen for IR, $\mu\text{-IR}$ and ATR spectroscopy measurements was cut.

Compression-moulded samples can be divided to three groups according to an analysing method that was applied after irradiation. Groups, applied analysing methods and thickness of analysed films are listed in Table 5.

Table 5. Groups of compression-moulded samples: Applied analysing methods and thickness of analysed films

Group	Method of analysing	Thickness of analysed films [μm]
1	FTIR spectroscopy	80, 180, 400, 500
2	$\mu\text{-IR}$ spectroscopy	180, 400
3	ATR spectroscopy	1000

7.2 Injection-moulded samples

From the polymer pellets standard impact testing bars (4 x 10 x 80 mm) were injection-moulded. The injection-moulded samples were prepared under processing conditions listed in Table 6.

Table 6. Processing conditions of the injection-moulded specimens

Mould temperature [°C]	60	Holding time [s]	40
Injection pressure [MPa]	65	Cooling time [s]	15
Injection speed [mm/s]	33	Cycle time [s]	100
Holding pressure [MPa]	65	-----	

8 ACCELERATED PHOTOAGEING

All samples of iPP were irradiated in a SEPAP 12.24 irradiation instrument at the temperature of 60 °C. This instrument has been described in chapter 4.

8.1 Compression-moulded samples

A table of irradiation times that were applied on Groups 1, 2 and 3 is given in Table 7.

Table 7. Table of applied irradiation times and irradiation conditions

Group	Times of irradiation [hours]	Conditions of irradiation *	Analyzing method
1	24, 48, 60, 70.58, 83.58, 96, 120, 144, 192	Non-covered	(FTIR)
2	70 hours 35 minutes (70.58 h)	Non-covered	(μ -IR)
	From both specimens a slice of irradiated material of thickness 15 μ m was cut perpendicularly to the oxidized surface using a microtome. Degradation profile through a sample was observed from the non-irradiated side.		
3	12, 24, 36, 60, 72, 96, 120, 132, 156, 172	Covered	(ATR)

(*) The conditions of irradiation say whether a back of the samples were covered by a piece of black paper during the irradiation.

8.2 Injection-moulded samples

Table 8. Table of applied irradiation times and irradiation conditions for injection-moulded samples

Sample	Times of irradiation [hours]	Conditions of irradiation *	Analyzing method
Testing bar	12, 24, 36, 60, 72, 96, 120, 132, 156, 172	Covered	(ATR)

9 ANALYSING METHODS AND DEVICES

Fourier transform infrared spectroscopy

Isotactic PP films of different thickness (in the range of 80–500 μm) were first irradiated in various irradiation times. Chemical changes for films were detected by FTIR spectroscopy. Films were studied by a spectrometer NICOLET Magma IR 760 (nominal resolution 4 cm^{-1} , 128 scans summation).

Attenuated total reflection infrared spectroscopy

Isotactic PP rectangular specimens were irradiated in various irradiation times. Samples were studied by ATR monoreflexion SPECAC with diamond crystal (nominal resolution 4 cm^{-1} , 128 scans summation).

Micro-infrared microscopy

Irradiated iPP specimens were studied by a spectrometer NICOLET Magma IR 760 (nominal resolution 4 cm^{-1} , 128 scans summation) coupled with microscope NIC-PLAN. This experimental arrangement is called a micro-infrared spectroscopy ($\mu\text{-IR}$). For these purposes, slices 15 μm thick were cut perpendiculary to the oxidized surface using microtome.

III. RESULT AND DISCUSSION

10 PHOTOCHEMICAL BEHAVIOUR OF FILMS HAVING DIFFERENT THICKNESS

The compression-moulded films with different thickness were exposed to UV radiation in accelerated laboratory conditions. After each irradiation time all films were studied by FTIR spectroscopy.

We obtained absorption spectra from which two absorption bands were the most important for this experiment – a carbonyl absorption band (from 1700 to 1800 cm^{-1}) and a reference absorption band (from 2700 to 2750 cm^{-1}).

The intensity of carbonyl absorption peak presents an amount of carbonyl photoproducts.

The shape of the carbonyl band is typically broad as it reflects several degradation products.

The absorption bands are generally ascribed to carbonyl by-products as convolutions of carboxylic acids, carbonyls, peresters and lactones [Čermák et al., 2005]. The evolution of infrared spectra in the region of carbonyl absorption is presented in Figure 15.

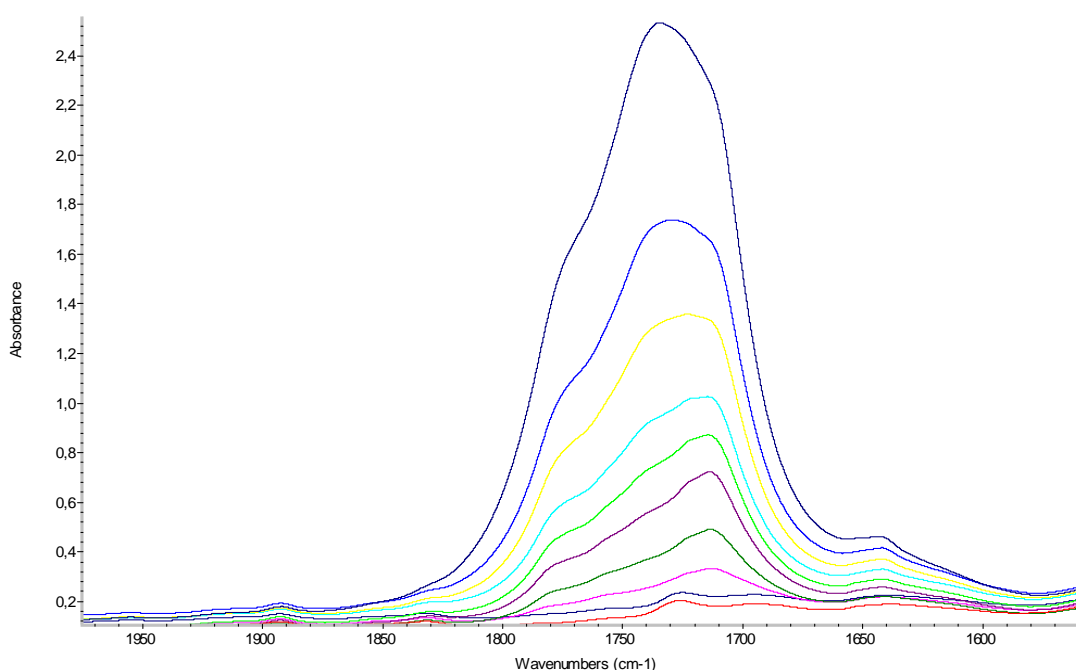


Figure 15. FTIR changes on photo-oxidation of iPP film of thickness about 180 μm in carbonyl vibration area. Irradiation at $\lambda > 300 \text{ nm}$ at 60 $^{\circ}\text{C}$ from 0 to 192 h

The reference absorption band associated with CH bending and CH₃ stretching is narrow, and it is affected neither by photo-oxidation nor by varying crystallinity. Moreover, it is not overlapped with other absorption bands. Therefore it is frequently used as reference. The intensity of reference absorption peak is proportional to the thickness of a sample. In Figure 16 the evolution of a reference and of a carbonyl absorption region of a film of thickness of 180 μm from 0 to 192 h is shown.

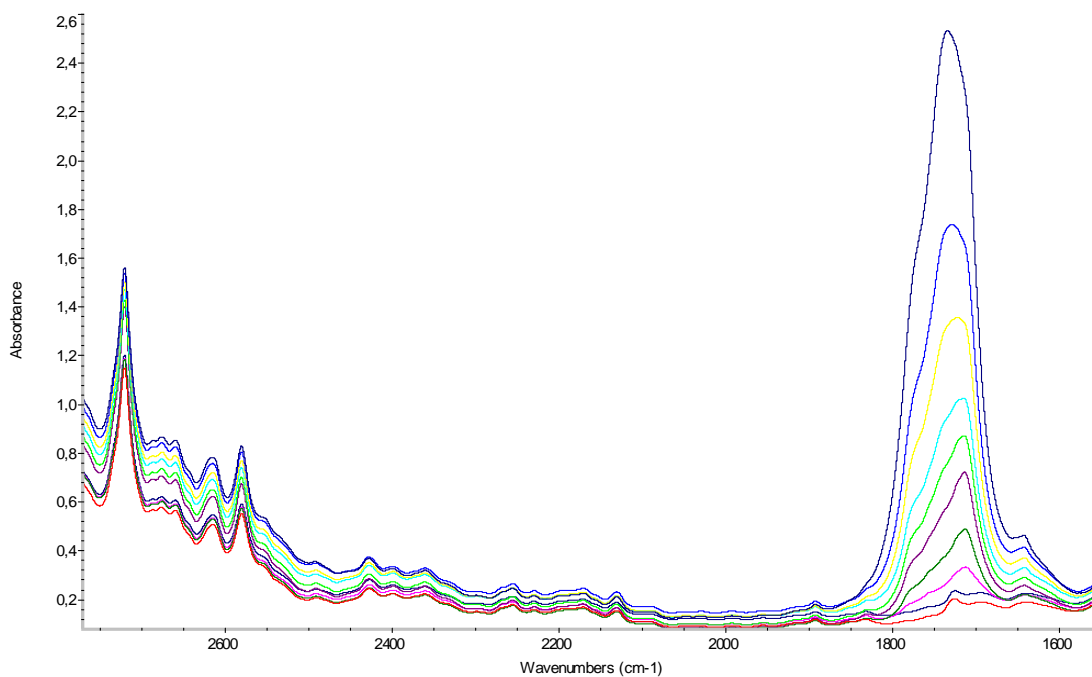


Figure 16. Absorption bands in the reference and carbonyl absorption area of iPP compression-moulded specimen of thickness 180 μm in different times from 0 to 192 h

Infrared spectra, which were obtained, were analysed by Nicolet OMNIC software.

Because some photoproducts in the carbonyl absorption area can be formed not only under direct experimental irradiation – they are formed in paucity in material in dependence on processing and storage conditions before the experiment – therefore, the intensity of carbonyl absorption peak in zero time was graphically – by using OMNIC software – subtracted from the intensity of carbonyl absorption peak in defined time:

$$A_{CO} = A_{CO}(t = x \text{ hours}) - A_{CO}(t = 0 \text{ hours}) \quad (11.1)$$

The result of the subtraction was used in Eq. 11.2 as the intensity of carbonyl absorption peak A_{CO} . Therefore, A_{CO} is in fact proportional to the amount of carbonyl photoproducts, which were formed only under irradiation at the experiment.

In Figure 17 the intensities of carbonyl absorption peaks A_{CO} (after subtraction) for various thicknesses of films are plotted as a function of irradiation time.

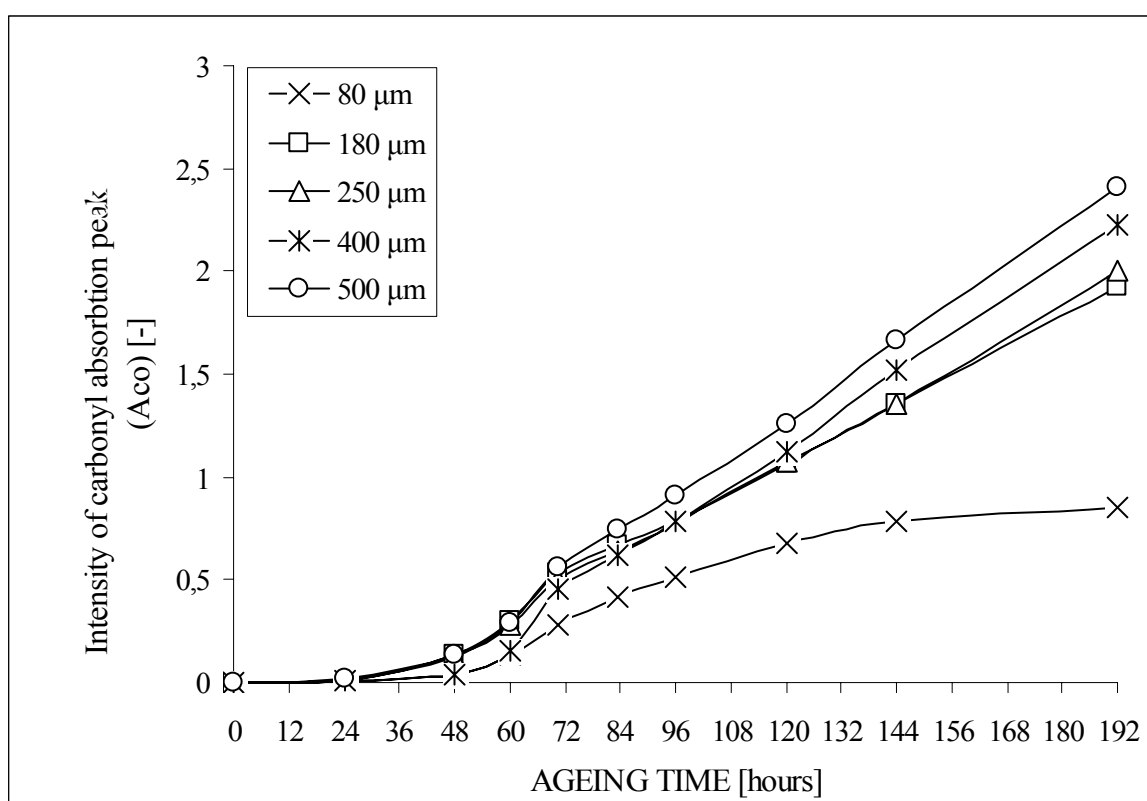


Figure 17. Intensity of carbonyl absorption peaks plotted as a function of ageing time

In Figure 17 no influence of the thickness is observed until about 24 h.

After 24 hours the kinetics of formation of carbonyl photoproducts of thin films is quite different from these of thick films. Significantly lower concentration of photoproducts in thin film can be assigned to lower portion of material that can undergo degradation process.

However, in general no influence of thickness of films is perceptible from Figure 17.

After 192 h of exposure, the thin film absorbance measured at 1720 cm^{-1} is divided by 2 and more in comparison with thick films as listed Table 9.

Table 9. Absorbance measured at 1720 cm^{-1} versus specimen thickness during photo-oxidation after 192 h

Thickness	80 μm	180 μm	250 μm	400 μm	500 μm
Absorbance	0.852	1.925	2	2.229	2.406

For quantified description of the degradation process the carbonyl index was used. It was calculated as the intensity of the carbonyl absorption peak A_{CO} (at 1720 cm^{-1}) related to the intensity of a reference peak A_{CH} (2750 cm^{-1}) as it is defined in Eq. 11.2:

$$\text{Carbonyl index} = \frac{A_{CO}}{A_{CH(\text{ref})}} \quad (11.2)$$

Figure 18 shows kinetic curves of the formation of carbonyl products upon photo-oxidation of iPP films of different thickness.

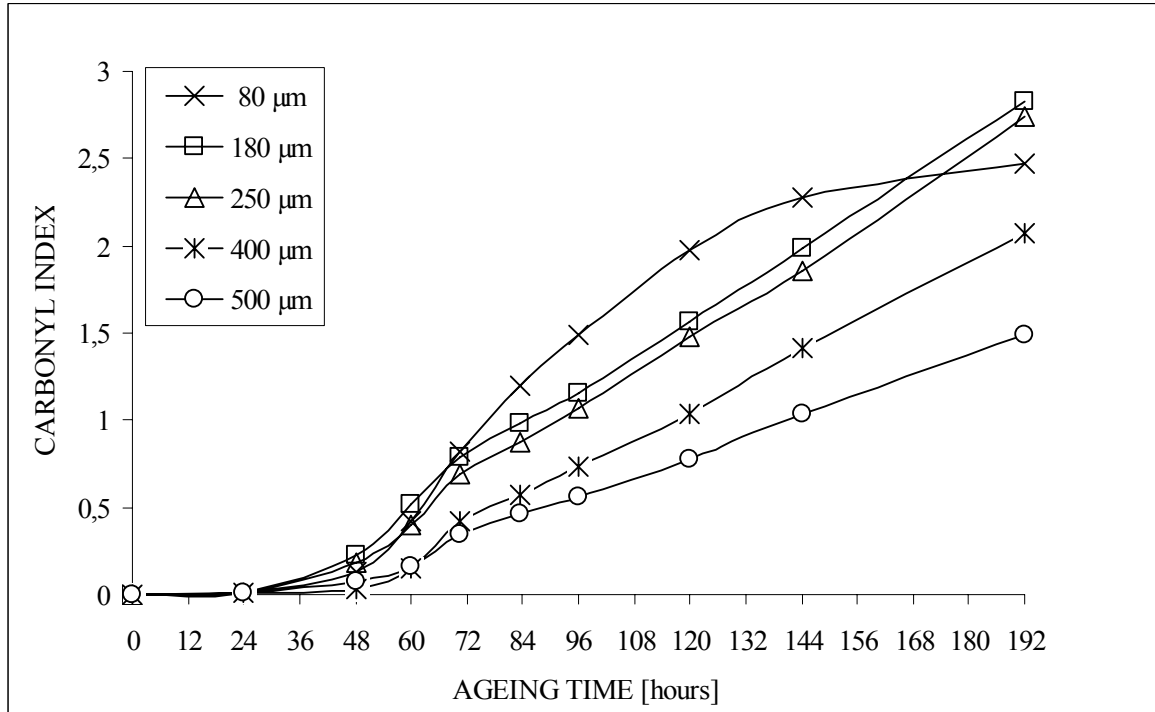


Figure 18. Effect of UV exposure on the carbonyl index of iPP films of different thickness

First, the induction period (defined as the time-lag during no photo-products is detected) seems to be similar and the initial oxidation rate appears to be independent of the film

thickness. After 24 hours the radical reaction accelerates and the differences between degradability of films of different thickness begin to be apparent.

The carbonyl absorption data become strongly thickness-dependent through the degradation period (after about 48 h of irradiation).

11 DEGRADATION PROFILE

Micro-infrared spectroscopy allows an examination of a degradation profile of thicker specimens, i. e. to define distribution of carbonyl photoproducts as a function of thickness.

Nevertheless, an analysis of first microns of specimens was difficult to provide because of consequences of oxidation and a microtome cut. The cut made by a microtome causes propagation of fissures and avulsion of first oxidized layers.

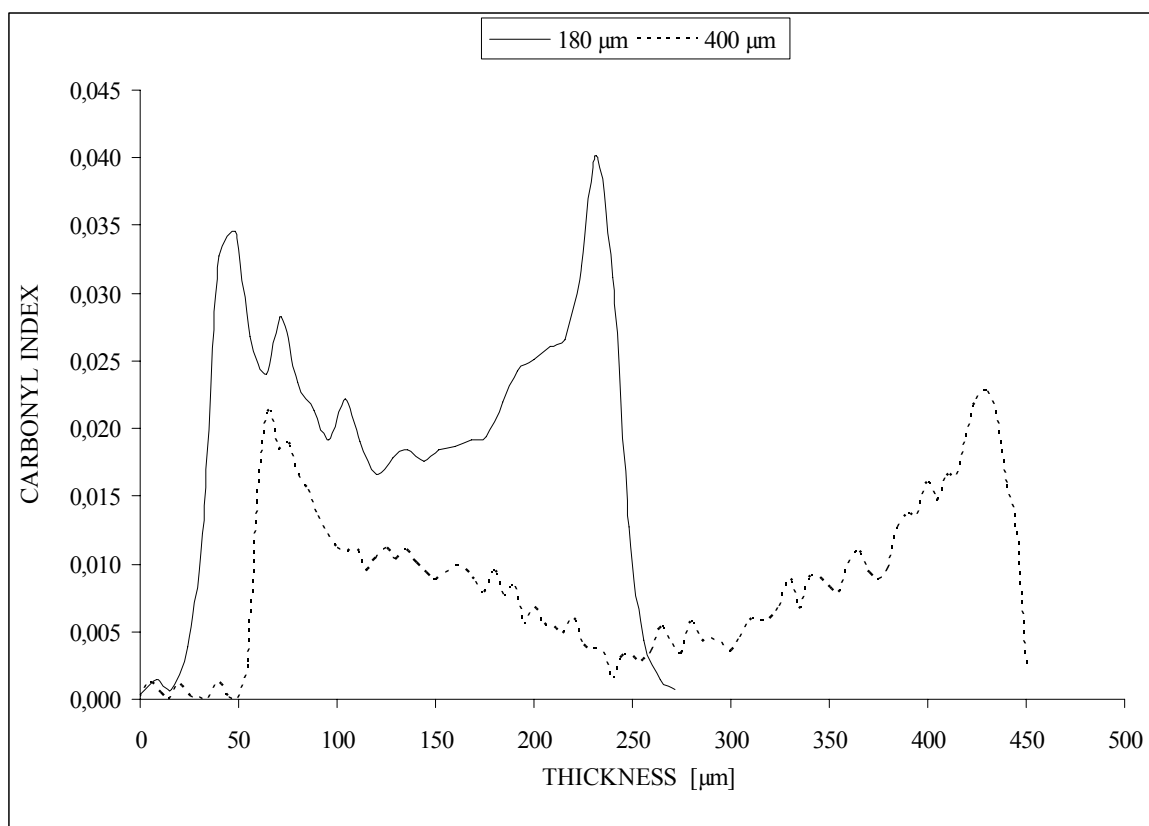


Figure 19. The effect of UV irradiation (approx. 70.5 h) and thickness on degradation profile of iPP specimens

Figure 19 shows the degradation profiles of iPP compression-moulded specimens and their relation to the thickness. Two samples of thickness 180 and 400 μm irradiated for approx. 70.5 h and after they were be observed by μ-IR spectroscopy from non-irradiated side.

Data were received directly from spectrometer NICOLET coupled with microscope NIC-PLAN.

Generally, a degradation profile shows how level of degradation, expressed by carbonyl index (i. e. an amount of photoproducts), is changed in dependence on thickness of specimen (i. e. through cross section of specimen).

In Figure 19 it can be seen that the oxidation in the surface layers is more apparent than that in the innermost layers. The carbonyl index decreases equally on both sides of specimen with increasing distance from the surface. In the centre area of the specimens the carbonyl indexes are the least significant. The photodegradation in the surface layers occurs more intensively than in the innermost layers.

As can be observed in Figure 19, the degradation profiles confirm heterogeneous distribution of carbonyl photoproducts.

From Figure 19 it is also apparent that the level of degradation drops with increasing specimen thickness. It results from an equation of carbonyl index where intensity of reference peak is dependent on thickness. Therefore, the influence of thickness is apparent if carbonyl index of specimens with different thickness are compared. It is possible to say that thicker specimen is less degraded towards its thickness than thinner specimen after same time of irradiation. It confirms the fact that the thickness of the specimen influence a lifetime of material.

As mentioned in the theoretical background, photodegradation is diffusion controlled and the oxidation rate increases with increasing oxygen permeability through the material. This process is significantly influenced by structural characteristics, in particular degree of crystallinity and molecular orientation. Therefore, the degradation profiles are subjected to the rules of oxygen diffusion and, thus, dependent on numerous material parameters such as permeability (morphology, chains orientation, crystallinity or structure of amorphous regions).

12 PROCESSING-INDUCED MORPHOLGY

Isotactic PP specimens were exposed to UV irradiation. We investigated how mode of processing affects photochemical behaviour of an injection-moulded (testing bar 4 x 10 x 80 mm) and a compression-moulded (film of 1000 μm) specimens. To investigate the surface layers, degradation extent was measured by ATR.

Obtained spectra were evaluated in the same way as spectra in a preceding experiment.

For intensity of carbonyl absorption peak a graphical subtraction was made as defined by Eq. 11.1. Degradation was characterized by carbonyl index that was calculated according to Eq. 11.2.

The evolution of IR spectra in the region of carbonyl absorption ($1700\text{--}1800\text{ cm}^{-1}$) is presented in Figure 20.

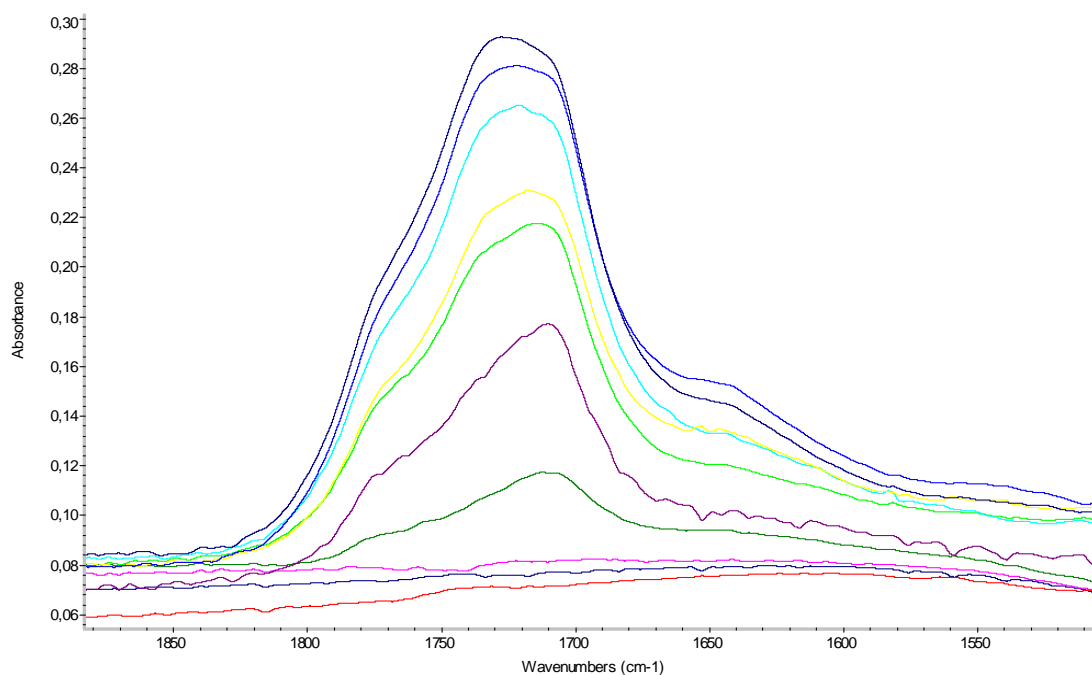


Figure 20. FTIR changes on photo-oxidation of iPP film of thickness about 1000 μm in carbonyl vibration area. Irradiation at $\lambda > 300\text{ nm}$ at 60 $^{\circ}\text{C}$ from 0 to 172 h. Spectra are displayed after subtraction in ascending order from 24 to 172h.

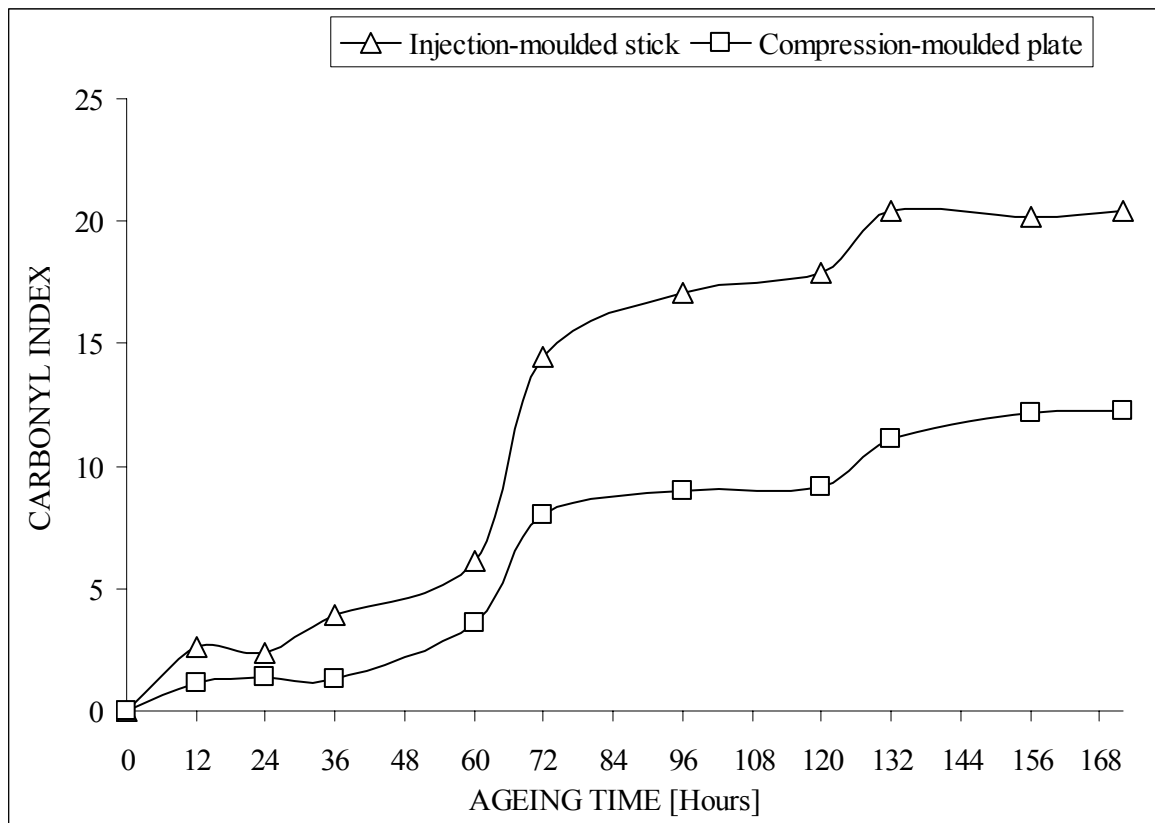


Figure 21. Effect of UV exposure on carbonyl index of compression- and injection-moulded specimen

Figure 21 shows the effect of the ageing on carbonyl index of compression- and injection-moulded specimens. What can be seen are different effects of UV radiation on the specimens. These different effects of UV exposure can be explained by different structural arrangements resulting from the mode of processing. The difference in crystal structure causes various photochemical behaviour during photo-degradation.

As described before in chapter 1.5 the flow effects during mould filling and thermodynamical gradients during solidification of the melt play a primary role during a formation of typical compression- or injection-moulded structure. Injection-moulded specimens possess a trilayer structure consisting of the non-spherulitic oriented skin, the intermediate region with conically shaped spherulites and the core with developed spherulities. The supermolecular architecture through the sample of compression-moulded polymer consists of two regions. For upper layer, cooling can lead to form conical spherulites. The innermost layer of specimen contains non-deformed spherulites.

Although both specimens were cooled at 60 °C, in the compression-moulded specimen cooling is slower. Temperature of a mould decreases slowly to 60 °C. Chains have more time to order, whereas chains in injection-moulded specimen are cooled immediately while touching the mould.

As it is evident from Figure 21, the effect of UV-exposure is substantially more pronounced for injection-moulded specimen and particularly evident at higher ageing times. Higher degradability of the injection-moulded sample reflects its particular morphology of surface layer, which is induced by flow during mould filling.

As oxygen diffusion to the polymer matrix controls a rate of photo-degradation process, the oriented surface layer of injection-moulded specimen probably simplifies oxygen diffusion.

As we supposed the surface layer of the sample which was injection-moulded is less stable under ultraviolet irradiation than that of the compression-moulded sample.

It can be assumed that processing and thermo-mechanical conditions during moulding of polymer significantly affect the structural development of polymers, and subsequently their susceptibility to photo-oxidation.

CONCLUSION

Isotactic polypropylene is one of the most common semicrystalline thermoplastics that exposed to UV-light tend to photo-oxidize. This master thesis deals with the effect of physical factors such as thickness or mode of processing on photochemical behaviour of isotactic polypropylene Mosten 58 412. Analysis of degradation profile was performed to confirm or disconfirm a hypothesis that the photo-oxidation occurs homogeneously.

An influence of thickness of irradiated compression-moulded specimens was investigated by Fourier transform infrared spectroscopy. It was found that an influence of thickness of analysed films on photo-oxidation is evident only if a level of degradation is expressed as carbonyl index. Actually, it means that the value of carbonyl index depends on material thickness. If the level of degradation is expressed as the intensity of carbonyl absorption peak the extent of degradation is not dependent on thickness. However, the thinnest film of 80 μm become to be less degraded after certain irradiation time. This is caused by total oxidation of specimen. Thus, it can be assumed that the thickness does not have direct influence on the extent of degradation.

A degradation profile was analysed by micro-infrared spectroscopy on irradiated compression-moulded specimens. The degradation profiles confirm heterogeneous distribution of carbonyl photoproducts through a cross section of the sample.

An influence of mode of processing was investigated by attenuated total reflection infrared spectroscopy by analysis of the surface layers of compression- and injection-moulded samples. It is recognized that the mode of processing and thermo-mechanical conditions during moulding of polymer significantly affect the structural development of polymers. Consequently, their susceptibility to photo-oxidation is affected. It was found that the surface layer of the sample which was injection-moulded is less stable under ultraviolet irradiation than that of the compression-moulded sample.

REFERENCES

- ADDINK, E. J., BIENTEMA, J.; *Polymer*, 2, 185, 1961.
- AL-RAHEIL, I. A., QUDAH, A. M., AL-SHARE, M.; *J. Appl. Polym. Sci.*, Vol. 67, 1259-1265, 1998.
- BARAN, N.; *Příprava β a γ fáze polypropylene: Dizertační práce*. FT, UTB, Zlín, 2001.
- BRÜCKNER, S., MEILLE, S.V.; *Nature*, 340, 455, 1989.
- ČERMÁK, R.; *Beta polypropylene: Interrelations between structure, properties and processing: Doctoral thesis*, FT, UTB, 2005.
- ČERMÁK, R., OBADAL, M., RAAB, M., VERNEY, V., COMMEREUC, S., FRAISSE, F.; Structure evolution of α - and β -polypropylenes upon UV irradiation: A multiscale comparison, *Polym. Degrad. Stabil.*, 88, 532-539, 2005.
- CHATANI, Y., MARUYAMA, H., NOGUCHI, K., ASANUMA, T., SHIOMURA, T.; *J. Polym. Sci.*, C28, 393, 1990.
- CHATANI, Y., MARUYAMA, H., ASANUMA, T., SHIOMURA, T.; *J. Polym. Sci.*, B29, 1649, 1991.
- CHENG, D. Z. S., JANIMAK, J. J., RODRIGUEZ, J.; *Polypropylene: Structure, blend and composites*, Vol. 2. *Crystalline structures of polypropylene homo- and copolymers*, Chapman&Hall, London, 1995.
- CORRADINI, P., NATTA, G., GANIS, P., TEMUSSI, P.A.; *J. Polym. Sci.*, C16, 2477, 1967.
- DOLEŽEL, B.; *Odolnost plastů a pryží*; SNTL, 1981.
- ELIAS, H. G.; *An Introduction to Plastics*, WILEY-VCH GmbH & Co.KGaA, Weinheim, 2003. ISBN 3-527-29602-6.
- FRIEDRICH, K.; *Adv. Polym. Sci.*, 52/53, 225, 1983.
- GRAVES, V.; *Polypropylene: A commodity Plastic Reaches Record Highs in 1994 Production*, *Modern Plastics Encyklopedia*. 1996.

- GROSSETETE, T.; *Etude de Polyolefines Recyclees a Haute Durabilite en Vue d'Applications Exterieures dans le Batiment*: These, Universite Blaise Pascal, Ecole Doctorale des Sciences Fondamentales, 2001.
- GUADAGNO, L., FONTANELLA, C., VITTORIA, V., LONGO, P.; Physical ageing of syndiotactic polypropylene, *J. Polym. Sci.: Part B: Pol. Phys.*, Vol. 37, 173-180, 1999.
- HAGEN, V.; *Únava a stárnutí polymerů*, VUT Brno, 76, 1977.
- JACOBY, P., BERSTED, B. H., KISSEL, W. J., SMITH, C. E.; Studies on β -crystalline form of isotactic polypropylene, *J. Polym. Sci. Pol. Phys.*, 24, 1986.
- KARGER-KOCSIS, J.; *Polypropylene – An A-Z Reference*. Kluwer Publishers, Dordrecht, 1999.
- KARGER-KOCSIS, J. , VARGA, J.; Effects of β - α transformation on the static and dynamic tensile behaviour of isotactic polypropylene., *J. Appl. Polym. Sci.*, 62, 291-300, 1996.
- KEITH, H. D., PADDEM, F. J., WALTER, N. M., WYCKOFF, H.W.; *J. Appl. Phys.*, 30, 1485, 1959.
- KRESSLER, J.; *Gamma-phase of isotactic polypropylene*. In KARGER-KOCSIS, J.; *Polypropylene – An A-Z Reference, 1st ed.* Dordrecht: Kluwer Academic Publishers, 267-272, 1999. ISBN 0-412-80200-7.
- LAPČÍK, L., RAAB, M.; *Nauka o materiálech II*. UTB, Zlín, 2004.
- LOTZ, B., LOVINGER, A. J., CAIS, R. E.; *Macromolecules*, 21, 2375.
- MAIER, C., CALAFUT, T.; *Polypropylene: The Definitive User's Guide and Databook*. Plastics Design Library, Norwich, NY, USA, 1998. ISBN 1-884207-58-8.
- MARK, S., M., ALGER; *Polymer science dictionary*. New York, 1989.
- MORROW, D. R., NEWMAN, B. A.; *J. Appl. Phys.*, 39, 4944, 1968.
- NATTA, G., CORRADINI, P.; *J. Polym. Sci.*, 39, 29, 1959.
- NATTA, G., CORRADINI, P.; *Suppl. Nuova Cimento*, 15, 40, 1960.
- NUNN, S., NISHIKIDA, K.; *Advanced ATR Correction Algorithm*, Thermo Electron Corporation, Madison, USA, 2003.

- OBADAL, M.; *Příprava polymerů s řízenou nadmolekulární strukturou: Doktorská disertační práce*. FT, UTB, Zlín, 2002.
- OBADAL, M.; *Asistovaná krystalizace polymerů: Habilitační práce*. FT, UTB, Zlín, 2005.
- OBADAL, M., ČERMÁK, R., RAAB, M., VERNEY, V., COMMEREUC, S., FRAISSE, F.; Study on photodegradation of injection-moulded β -polypropylenes, *Polym. Degrad. Stabil.*, Elsevier Ltd, 459-463, 2005.
- OSSWALD, T., A., MENGES, G.; *Material science of polymers for engineers*. Hanser, 622, Munich, 2003.
- PADDEN, F.J., KEITH, H.D.; *J. Appl. Phys.*, 30, 1479, 1959.
- PHILLIPS, P. J., MEZGHANI, K.; *Polypropylene, isotactic (Polymorphism)*, Department of Materials Science and Engineering University of Tennessee, 1996.
- PHILIPS, R.A., WOLKOWICZ, M. D.; *Structure and morphology, Polypropylene handbook, reference book*. Carl Hanser, Verlag, 1996. ISBN 3-446-18176-8.
- ROSATO, DOMINICK. V., ROSATO, DONALD V., ROSATO, M.V.; *Plastics Products Material and Process Selection Handbook*, Elsevier, 2004. ISBN 1-85617-431-X.
- SCHNABEL, W.; *Polymer Degradation, Principles and practical Application*, Hanser, Wien, 1981.
- SHAN, V.; *Handbook of Plastics Testing Technology, 2nd ed.* A Wiley-Interscience publication, USA, 1998. ISBN 0-471-18202-8.
- SARWADE, B. D., SINGH, R. P.; *J. Appl. Polym. Sci.*, 72, 215, 1999.
- SUETAKA, K. I.; *Surface IR & Raman spectroscopy: method and application*; New York: Plenum, 1995.
- TURNER-JONES, A., AIZLEWOOD, J. M., BECKETT, D. R.; *Macromol. Chem.*, 75, 134, 1964.
- VARGA, J.; *Crystallization, melting and supermolecular structure of isotactic polypropylene, in Polypropylene: Structure, Blends and Composites, Vol.*

I., Structure and Morphology (ed. KARGER-KOCSIS, J.), Chapman&Hall, London, 56-115,1995.

VARGA, J.; β -modification of isotactic polypropylene: preparation, structure, processing, properties, and application, *J. Macromol. Sci.*, Vol. 41, 1121-1171, 2002.

WANG, Z., WANG, X., HSIAO B. S., PHILLIPS, R. A., MEDELLIN-RODRIGUEZ F. J., SRINIVAS, S., WANG, H., HAN CH. C.; Structure and morphology development in syndiotactic polypropylene during isothermal crystallization and subsequent melting, *J Polym. Sci.: Part B: Pol Phys.*, Vol. 39, 2982-2995, 2001.

WHITE, J. L.; CHOI, D. D.; *Polyolefins: Processing, Structure Development, & Properties*. Carl Hanser Verlag, Munich, 2005.

WOODWARD, A. E.; *Understanding polymer morphology*. Hanser/Gardner Publication, Cincinnati, Ohio, USA, 1995. ISBN 3-446-17431-1.

ZHENG, Q., SHANGGUAN, Y., TONG, L., PENG, M.; Effect of vibration on crystal morphology and structure of isotactic polypropylene in non-isothermal crystallization *J. Appl. Polym. Sci.*, Vol. 94, 2187-2195, 2004.

www 1: Polypropylene [cit. 2007-02-14]. Available on WWW:

<<http://www.pslc.ws/mactest/pp.htm>>.

www 2: General Chemistry : Chapter 15B. Molecular Spectroscopy 1996-10-11: Infrared spectroscopy [cit. 2007-02-20]. Available on WWW:

<<http://www.wag.caltech.edu/home/jang/genchem/infrared.htm>>.

www 3: Wikipedia: The Free Encyclopedia: Electromagnetic radiation [cit.2007-02-20].

Available on WWW:

<http://en.wikipedia.org/wiki/Electromagnetic_radiation>.

www 4: Wikipedia: The Free Encyclopedia: Planck's constant [cit. 2007-02-21]. Available on WWW:

<http://en.wikipedia.org/wiki/Planck%E2%80%99s_Constant>.

www 5: Wikipedia: The Free Encyclopedia: Fluorescence [cit.2007-02-21]. Available on

WWW: <<http://en.wikipedia.org/wiki/Fluorescence>>.

www 6: Wikipedia: The Free Encyclopedia: Phosphorescence [cit. 2007-02-21]. Available on WWW: <<http://en.wikipedia.org/wiki/Phosphorescence>>.

www 7: CNEP France [cit. 2007-04-12]. Available on WWW:

<<http://www.cnep-ubp.com/>>.

www8 : TI 110-18 SEPAP Test Information. PDF [cit. 200-04-12]. Available on WWW:

<<http://www.pes-tec.com/pdf/TI%20110-18%20SEPAP%20Test%20Informations.pdf>>.

www 9: Wikipedia: The Free Encyclopedia: Infrared spectroscopy [cit. 2007-02-20].

Available on WWW:

<http://en.wikipedia.org/wiki/Infrared_spectroscopy>.

www 10: The Science of Spectroscopy [cit. 2007-02-20]. Available on WWW:

<http://scienceofspectroscopy.info/edit/index.php?title=Infrared_Spectroscopy>.

www 11: VŠCHT Infračervená spektroskopie [cit. 2007-02-10]. Available on WWW:

<<http://lms.vscht.cz/Zverze/Infrared.htm>>.

www 12: : Wikipedia: The Free Encyclopedia: Fourier Transform Spectroscopy [cit. 2007-03-08]. Available on WWW:

<http://en.wikipedia.org/wiki/Fourier_transform_spectroscopy>.

www 13: WCAS FTIR [cit. 2007-03-10]. Available on WWW:

<<http://www.wcaslab.com/tech/tbftir.htm>>.

www 14: TCH_FTIRATR.PDF [cit. 2007-03-12]. Available on WWW:

<http://las.perkinelmer.com/content/TechnicalInfo/TCH_FTIRATR.pdf>.

www 15: Wikipedia: The Free Encyclopedia: ATR Spectroscopy [cit. 2007-03-08].

Available on WWW:

<http://en.wikipedia.org/wiki/Attenuated_total_reflectance>.

LIST OF SYMBOLS AND SHORTCUTS

PP	Polypropylene
iPP	Isotactic polypropylene
aPP	Atactic polypropylene
sPP	Syndiotactic polypropylene
T_m [°C]	Melting temperature
λ [m]	Wavelength
c [m/s]	Speed of light
h [J.s]	Planck's constant
E [J]	Energy of photon
S_0	Ground state of molecule
S_1	Excited state of molecule
T_1	Triplet state of molecule
IR	Infrared
I [-]	Intensity of light passed through the sample
I_0 [-]	Intensity of light coming out of the source
T [%]	Transmittance
A [-]	Absorbance
FTIR	Fourier transform infrared spectroscopy
ATR	Attenuated total reflection spectroscopy
μ -IR	Micro-infrared
d_p [μm]	Analysed thickness
n_1 [-]	Refractive index of a crystal
n_2 [-]	Refractive index of a sample
Φ [°]	Incidence angle

LIST OF FIGURES

Figure 1. Polymerisation reactions of propylene units [www 1].....	10
Figure 2. One mer unit of the propylene macromolecular chain [www 1].....	10
Figure 3. Atactic polypropylene structure [Osswald and Menges, 2003]	11
Figure 4. Syndiotactic polypropylene structure [Osswald and Menges, 2003].....	12
Figure 5. Isotactic polypropylene structure [Osswald and Menges, 2003]	13
Figure 6. Four possible arrangements of the iPP chain in a crystal lattice [Karger-Kocsis, 1999].....	14
Figure 7. The diffraction spectra of crystalline α , β and γ forms of iPP [Obadal, 2002]....	15
Figure 8. Crystal structure of α -form of iPP [Karger-Kocsis, 1999].....	16
Figure 9. The trigonal unit cell of β -form of iPP [Addink and Bientema, 1961]	17
Figure 10. Structure of injection-moulded sample skin-intermediate-core [Woodward, 1995].....	21
Figure 11. Electromagnetic spectrum [www 2].....	24
Figure 12. Accelerated ageing device SEPAP 12.12 [www 7]	32
Figure 13. Infrared spectroscopy correlation table [www 9].....	33
Figure 14. Attenuated total reflection infrared spectroscopy accessory [www 13]	35
Figure 15. FTIR changes on photo-oxidation of iPP film of thickness about 180 μm in carbonyl vibration area. Irradiation at $\lambda > 300$ nm at 60 $^{\circ}\text{C}$ from 0 to 192 h.....	45
Figure 16. Absorption bands in the reference and carbonyl absorption area of iPP compression-moulded specimen of thickness 180 μm in different times from 0 to 192 h.....	46
Figure 17. Intensity of carbonyl absorption peaks plotted as a function of ageing time.....	47
Figure 18. Effect of UV exposure on the carbonyl index of iPP films of different thickness	48
Figure 19. The effect of UV irradiation (approx. 70.5 h) and thickness on degradation profile of iPP specimens.....	50
Figure 20. FTIR changes on photo-oxidation of iPP film of thickness about 1000 μm in carbonyl vibration area. Irradiation at $\lambda > 300$ nm at 60 $^{\circ}\text{C}$ from 0 to 172 h. Spectra are displayed after subtraction in ascending order from 24 to 172h.	52
Figure 21. Effect of UV exposure on carbonyl index of compression- and injection-moulded specimen.....	53

LIST OF TABLES

Table 1. The unit cells parameters of sPP crystalline forms [White and Choi, 2005].....	12
Table 2. The unit cells parameters of iPP crystalline forms [White and Choi, 2005].....	15
Table 3. Relative weather resistances of unmodified thermoplastics [Shan, 1998].	23
Table 4. Factors affecting resistance of material to photodegradation [Grossetete, 2001].....	27
Table 5. Groups of compression-moulded samples: Applied analysing methods and thicknesses of analysed films	40
Table 6. Processing conditions of the injection-moulded specimens	41
Table 7. Table of applied irradiation times and irradiation conditions	42
Table 8. Table of applied irradiation times and irradiation conditions for injection-moulded samples	42
Table 9. Absorbance measured at 1720 cm^{-1} versus specimen thickness during photo-oxidation after 192 h.....	48

